doi:10.1093/brain/awh604 *Brain* (2005), **128,** 2338–2358

Performance of locomotion and foot grasping following a unilateral thoracic corticospinal tract lesion in monkeys (*Macaca mulatta*)

Grégoire Courtine,[1] Roland R. Roy,[3] Joseph Raven,[1] John Hodgson,[1,3] Heather Mckay,[4] Hong Yang,[5] Hui Zhong,[1] Mark H. Tuszynski[5,6] and V. Reggie Edgerton[1,2]

[1]Department of Physiological Science, [2]Department of Neurobiology and [3]Brain Research Institute, University of California, Los Angeles, [4]California Regional Primate Research Center, University of California, Davis, [5]Department of Neurosciences, University of California, San Diego, La Jolla and [6]Veterans Administration Medical Center, San Diego, CA, USA

Correspondence to: V. Reggie Edgerton, PhD, Department of Physiological Science, University of California, Los Angeles, 621 Charles E. Young Drive South, Los Angeles, CA 90095-1527, USA
E-mail: vre@ucla.edu

Six adult monkeys (*Macaca mulatta*) received a unilateral lesion of the lateral corticospinal tract (CST) in the thoracic spinal cord. Prior to surgery, the animals were trained to perform quadrupedal stepping on a treadmill, and item retrieval with the foot. Whole body kinematics and electromyogram (EMG) recordings were made prior to, and at regular intervals over a period of 12 weeks after the CST lesion. After 1 week of recovery, all monkeys were able to walk unaided quadrupedally on the treadmill. The animals, however, dragged the hindpaw ipsilateral to the lesion along the treadmill belt during the swing phase and showed a significant reorganization of the spatiotemporal pattern of hindlimb (HL) and forelimb (FL) displacements. The inability to appropriately trigger the swing phase resulted in an increase in the cycle duration and stride length of both HLs. The stance duration decreased in the ipsilateral HL, and increased in the contralateral HL and both FLs. Consequently, there was a dramatic disruption of interlimb and intralimb coupling that was reflected in the limb kinematic and EMG patterns. The CST lesion completely abolished the ability of the monkeys to retrieve items with the foot ipsilateral to the lesion and significantly disrupted the level of performance of the contralateral HL during the first 2 weeks post-lesion. Interestingly, selected HL muscles remained almost quiescent when the monkeys attempted to retrieve items, but were unsuccessful with the affected foot at 1 week post-lesion, whereas the capacity to activate the same muscles was preserved, although reduced, during stepping. Spatial and temporal parameters of gait, kinematics, and EMG patterns recorded during locomotion generally converged toward control values over time, but significant differences persisted up to 12 weeks post-lesion. Although some control was recovered over the distal foot musculature, fine foot grasping remained significantly impaired at the end of the testing period. These findings demonstrate that the CST pathway from the brain normally makes an important contribution to interlimb and intralimb coordination during basic locomotion, and to muscle activation to produce dexterous foot digit movements in the monkey. Furthermore, the present study indicates that the primate has the ability to rapidly accommodate locomotor performance, and to a lesser degree fine foot motor skills, to a reduction in supraspinal control. Identification of the neural substrates mediating the rapid recovery of motor function following injury to the primate spinal cord could provide insight into developing repair strategies to augment functional recovery from neuromotor impairments.

Keywords: corticospinal pathways; foot grasping; locomotion; monkey; spinal cord injury

Abbreviations: CST = corticospinal tract; FL = forelimb; SCI = spinal cord injury; PC = principal component; HL = hindlimb; MCP = metacarpo-phalangeal; LE = lower extremity; MTP = metatarso-phalangeal

Received February 2, 2005. Revised June 28, 2005. Accepted June 30, 2005. Advance Access publication July 27, 2005

Introduction

Spinal cord injury (SCI) is a major source of morbidity worldwide, with the loss of ambulation and fine motor movements being among the most devastating consequences of such an injury (Anderson, 2004). Recent progress has been made in understanding the mechanisms and consequences of injury to the CNS, and in augmenting CNS plasticity and regeneration after experimental SCI in sub-primate mammals (Jones *et al.*, 2001; Edgerton and Roy, 2002; Schwab, 2002). Nevertheless, the relevance of this work to injured primate systems, including humans, may depend upon the extent of the similarities in the anatomical and functional organization of the sensorimotor systems between lower and higher order mammals (Tuszynski *et al.*, 2002), as well as the motor task in question, i.e. locomotion versus fine motor tasks.

There are relatively few data on the organization of the neural control mechanisms involved in the generation of walking in the non-human primate (Mori *et al.*, 1996; Duysens and Van de Crommert, 1998; Recktenwald *et al.*, 1999; Nakajima *et al.*, 2004; Courtine *et al.*, 2005). Although the few studies performed in monkeys emphasize that activation of stepping-related spinal circuits depends more on supraspinal input in non-human primates than in sub-primate mammals (Eidelberg *et al.*, 1981; Fedirchuk *et al.*, 1998; Vilensky and O'Connor, 1998), quantitative assessments of the degree of supraspinal control of locomotion in primate species has been minimal. In comparisons with other mammals, the emergence of direct cortical projections to both cervical and lumbar motor neurons is one of the most intriguing neuro-anatomical aspects of primate evolution (Kuypers, 1981; Galea and Darian-Smith, 1997*a*; Lacroix *et al.*, 2004; Lemon *et al.*, 2004). A relevant feature to consider, thus, is whether the massive cortical projections to the spinal cord in primates correlate with an increased contribution to bipedal walking, and to the performance of dexterous tasks with the hindlimbs (HLs).

Lesion of the pyramidal or corticospinal tract (CST) has little or no effect on stepping over a flat surface in rodents (Muir and Whishaw, 1999) and cats (Liddell and Phillips, 1944) 1–2 weeks after a lesion is induced, indicating that the motor cortex is not an essential structure for creating the muscle synergies sustaining simple locomotion in these species. Likewise, the remarkable recovery of locomotor function observed in monkeys (Tower, 1940; Lawrence and Kuypers, 1968*a*) following selective interruption of the pyramidal pathways suggests that cortical input is not essential for the generation of basic locomotor movements in non-human primates. Such an extensive recovery, however, does not imply *per se* that the motor cortex makes no significant contribution to the locomotor drive under normal conditions, as demonstrated in the walking cat (Drew *et al.*, 2002; Bretzner and Drew, 2005). Indeed, the acute impairments in muscle activity and gait movements have not been quantified under stereotypical walking conditions and, therefore, the amount of recovery from locomotor deficits remains unclear in monkeys (Tower, 1940; Lawrence and Kuypers, 1968*a*). Furthermore, in the perspective of SCI research, it becomes important to compare the motor deficits resulting from interruption of the CST projections in monkeys with respect to humans. In fact, in contrast to non-human primates, neurological reports reveal that damage to the CST in the human spinal cord (Nathan, 1994) leads to paresis or flaccid paralysis of the legs, and thereby permanently abolishes the ability to walk independently. Moreover, transcranial magnetic stimulation (Capaday *et al.*, 1999; Petersen *et al.*, 2001) and brain imaging (Fukuyama *et al.*, 1997; Miyai *et al.*, 2001; Bonnard *et al.*, 2002) investigations are demonstrating the involvement of supraspinal structures in the production of human locomotion.

In the present study, we have examined in considerable detail the effects of a unilateral lesion of the CST at a low thoracic spinal cord level on the quadrupedal stepping ability of monkeys (*Macaca mulatta*). Longitudinal recordings of whole body movements and muscle activity using chronically-implanted EMG electrodes before and after injury allowed us to detail the initial deficits resulting from the lack of cortical input from one cerebral hemisphere on locomotor performance, and to assess the degree of spontaneous recovery in walking ability following a unilateral thoracic CST lesion.

Furthermore, we compared the deficits in quadrupedal stepping of monkeys with their ability to perform a fine motor task involving dexterous foot digit movements. Previous studies have shown that the development of the descending pathways from the brain in primates directly correlates with the ability to perform fractionated movements of hand distal extremities, i.e. manual dexterity (Lawrence and Kuypers, 1968*a*; Galea and Darian-Smith, 1997*b*; Lemon *et al.*, 2004; Sasaki *et al.*, 2004). The contribution of cortical input in the production of skilled foot movements, however, has not been elucidated. Dexterous grasping with the foot is a key feature in the successful adaptation of non-human primates to an arboreal environment (Schmitt, 2003). It seems important, therefore, to identify whether the massive cortical projections to lumbar ventral horn neurons in monkeys compared to rodents and cats (Lacroix *et al.*, 2004) are associated with the emergence of fine foot grasping ability of monkeys, as well as to compare the effects of a CST lesion on the generation of locomotion versus fine motor tasks. On the basis of previous reports (Lawrence and Kuypers, 1968*a*), we hypothesize (i) that thoracic interruption of the CST projections would significantly disrupt locomotion and fine foot motor control in monkeys; and (ii) that there would be a near-complete recovery of quadrupedal stepping ability within a period of weeks, whereas impairment of dexterous foot grasping would persist.

Our results show that cortical input in monkeys normally makes a significant contribution to the level of intralimb and interlimb coordination during quadrupedal stepping, and to the activation of HL muscles to produce dexterous foot movements. Our findings, however, highlight the ability of

the primate CNS to accommodate rapidly to the reduction in supraspinal control for the successful generation of locomotion, and to a lesser extent, fine foot motor skills. These results have significant implications regarding the descending control of the spinal motor mechanisms and its potential plasticity in primates, including humans, and may provide a guide for developing rehabilitation strategies to enhance recovery following SCI. A portion of these results has been published in abstract form (Courtine *et al.*, 2004).

Materials and methods

Experimental subjects and motor tasks

Subjects

Six adult male monkeys (*M.mulatta*) were studied (mean age 7 years; Table 1). All surgical and experimental procedures in these experiments were carried out using the principles outlined by the Laboratory Animal Care (National Institutes of Health Publication 85–23, revised 1985) and were approved by the Institutional Animal Care and Use Committee (IACUC). Each animal was trained for a minimum of 1 month to perform quadrupedal locomotion on a treadmill and a fine grasping task with the foot.

Treadmill training

The six monkeys were trained to walk quadrupedally on a motor-driven treadmill. A Plexiglas enclosure was used to maintain the animal in position while allowing video recording of their movements. The initial training sessions were used to acclimate the animals to the treadmill environment without the belt moving. Subsequent sessions were used to train the animals to locomote consistently at speeds of 0.45, 0.89, 1.34 and 1.79 m/s. Each training session consisted of eight locomotor trials (two repetitions at each speed) with approximately a 1 min rest period between each trial. The duration of each session was ~40 min. A variety of food items were used as rewards after each locomotor trial.

Foot grasping task

To examine lower extremity manual dexterity, a skilled motor task thought to reflect the functional integrity of the corticospinal projection to the HLs (Lawrence and Kuypers, 1968*a*; Galea and Darian-Smith, 1997*b*; Lemon *et al.*, 2004; Sasaki *et al.*, 2004) was used. Subjects were chair trained and their behaviour was shaped over several subsequent sessions to retrieve food rewards of three sizes with each foot independently. The monkeys were presented either with a raisin (10 trials/session, two consecutive daily sessions per week), a grape (10 trials/session, two consecutive daily sessions per week), or a 1/24 apple slice (5 trials/session, two consecutive daily sessions per week) and the number of successful food retrievals was recorded for each session (see below).

Surgical procedures

The monkeys were housed individually in standard 4.3 or 6.1 square feet stainless steel cages. The monkeys were housed and all surgical procedures were performed at the California National Primate Research Center (CNPRC, University of California, Davis, CA, USA). The following anaesthesia regimen was followed. Pre-operative management consisted of food restriction for ~8 h. Induction of anaesthesia was with ketamine HCl (10 mg/kg i.m.). Atropine sulphate (0.04 mg/kg i.m.) was administered during induction. A catheter was placed in either the saphenous or cephalic vein to supply fluids during the procedure, and a tracheal tube was placed to give a free airway for gas anaesthesia. Anaesthesia was maintained with isoflurane gas (1.25%) in 100% oxygen delivered via a cuffed orotracheal tube. Throughout the surgery, a trained animal health technician monitored heart rate, blood pressure, O_2 saturation, CO_2 expiration levels, core body temperature, respiratory rate, respiratory pressure and tidal volume using a surgical Ohmeda-Datex unit. Lactated Ringer solution (10 ml/kg/h) was administered at a continuous infusion rate for the duration of anesthesia. Prior to any incisions being made, the depth of anaesthesia was assessed by checking heart rate, blood pressure, jaw tone and toe-pinch response. Adjustments in the level of anaesthesia were made as needed. Analgesia was provided by either oxymorphone (0.15 mg/kg, i.m., TID) or Buprenex (0.5–1.0 mg/kg i.m., TID). The analgesics were initiated prior to completion of the surgery and continued for a minimum of 3–5 days. The monkeys were monitored closely for food and water intake and were supplemented liberally with fresh fruit and vegetables on a daily basis until their normal appetite resumed. Antibiotic therapy with cephazolin (20 mg/kg i.m., TID) or cephalexin (30 mg/kg, oral, BID) was initiated pre-operatively (given every 2 h during the procedure) and continued for 5–10 days.

EMG implants

After the training period, two (#1 and #2) monkeys were implanted with bipolar intramuscular EMG electrodes into selected muscles under aseptic conditions. EMG electrode arrays similar to those described by Hodgson *et al.* (2001) were purchased from a commercial source (Model TK-12, Konigsberg Instruments, Pasadena, CA, USA). Table 2 identifies the muscles implanted in each monkey, and lists the main actions of each muscle as well as the muscle abbreviations used throughout the text. The electrode implant procedures

Table 1 Body weight, age, spinal cord level and side on which the lesion was performed, total mean numbers (±SEM) of BDA-labelled CST axons one spinal segment rostral and one segment caudal to the lesion, and lesion completeness for each monkey

Monkey	Age	Body weight (kg)	Level	Side	Rostral	Caudal	Lesion completeness (%)
#1	7 years and 3 months	10.1	T10	Right	See text		95
#2	15 years	13.9	T3	Right	1070 ± 41	248 ± 1.4	77
#3	4 years and 2 month	6.7	T10	Left	269 ± 16.1	2.33 ± 0.9	99
#4	8 years and 2 months	10.0	T10	Left	374 ± 10.8	6.67 ± 0.7	98
#5	6 years and 5 months	9.9	T10	Left	365 ± 13	90 ± 1.7	75
#6	4 years and 2 months	6.4	T10	Right	489 ± 20.5	316 ± 6.1	35

Table 2 Summary of muscles studied and their primary actions

Implanted muscles	Abb.	Main action	Monkey
Vastus lateralis	VL	Knee extension	#1 (LR)
Medial gastrocnemius	MG	Plantarflexion/knee flexion	#1, #2 (all LR)
Soleus	Sol	Plantarflexion	#1 (LR), #2 (R)
Tibialis anterior	TA	Dorsiflexion/inversion	#1 (LR)
Flexor digitorum longus	FDL	2nd–5th toes flexion/weak plantarflexion	#2 (R)
Flexor hallucis longus	FHL	Big toe flexion/plantarflexion	#2 (R)

L, left; R, right; Abb., abbreviations.

have been described in detail previously (Courtine *et al.*, 2005). Post-operative care consisted of intensive monitoring until the monkeys regained their equilibrium and were able to sit upright. Wound healing was monitored closely by dedicated veterinary and therapeutics staff. Initial care immediately after surgery consisted of monitoring the transcutaneous exit sites for erythema or exudation. If deterioration of the exit sites was noted, the incision sites were cleansed with dilute Novalsan solution (chlorohexidine) and topical antibiotics were used if deemed necessary by the veterinary staff. If necessary, systemic antibiotic therapy was initiated with the drug of choice from the case veterinarian.

Spinal cord lesion

To create T10 CST lesions, the level for laminectomy was identified by palpating rostrally from the T12 posterior spinous process. A dorsal skin incision was placed over the identified T10 region and a dorsal laminectomy was performed, exposing the spinal canal. A Kopf microwire lesion knife (General Valve, Fairfield, NJ) was positioned 0.5 mm lateral to the spinal cord midline on the lesioned side (Table 1), and was lowered to a depth of 2 mm into the cord through a small dural incision. The wire knife then was extruded creating a final targeted lesion dimension of 5 mm depth × 5 mm width. The knife was raised through the cord with the arc extruded, thereby transecting all structures falling within the arc. Lesion completeness was assured by placing direct pressure with a blunt jeweller's forceps on the extruded wire knife during the lesion procedure, visually verifying the absence of fibres. This procedure was repeated a second time in the same location. Muscle and skin layers then were sutured in layers. Unilateral corticospinal lesions were utilized because they spare autonomic function, facilitating post-operative management of lesioned subjects. Bowel and bladder function were not compromised by this lesion. Post-operatively, the monkeys were supported and provided analgesics for 3–5 days and antibiotics for 5–7 days as described above.

Tracer injection

For microinjections of the neuronal tracer biotin dextran amine (BDA) (10 000 molecular weight, Molecular Probes, Eugene, OR), a craniotomy was performed to expose the primary motor cortex contralateral to the lesion side, as previously described (Lacroix *et al.*, 2004). Tracer injections were placed into the hemisphere contralateral to the lesion side to examine bilateral projection patterns of the CST for related anatomical studies (not described in this report). BDA injections were performed 3 weeks prior to sacrifice. A total of 126 tracer injections per monkey were made. Anterograde tracing methods were used to assess lesion completeness, and to allow future anatomical study of corticospinal axon responses to transection. For purposes of the present study, tracer injections focused primarily on projections from the lower extremity (LE) cortex to the lumbar spinal cord. A total of 126 tracer injections per monkey were targeted to layer V of the primary and supplementary motor cortex regions projecting to the LE. A quantity of 280 nl of a 10% solution of BDA was injected into each site over 15 s through a pulled glass micropipette (outer diameter of 40 μm) using a picospritzer (General Valve, Inc.) that delivered 30 nl/pulse. Stereotaxic injection sites were established by measuring coordinates of the falx cerebri and injecting a series of sites spanning the entire LE as described in detail in Lacroix *et al.* (2004). Based on previous electrophysiological and anatomical studies (Galea and Darian-Smith, 1994), these boundaries include the vast majority of the primary motor cortex that projects to the LE region. Some overlapping projections originating from premotor areas, including the caudal component of the supplementary motor area and cingulate motor areas, would be included in these boundaries. After completing injections, the craniotomy site was closed by replacing the skull flap. Subjects were perfused 9–12 weeks after tracer injections for visualization of labelled axons.

Tissue processing and histology

Monkeys were deeply sedated with ketamine (10 mg/kg i.m.) and deeply anaesthetized with sodium pentobarbitol (∼60 mg/kg, i.v.). All reflex responses to cutaneous stimulation were verifiably absent before transcardial perfusion for 2 h starting with 1% paraformaldehyde for 10 min, followed with 4% paraformaldehyde in 0.1 M phosphate buffer (pH 7.4) at 4°C, and then post-fixed in 4% paraformaldehyde, 10% glycerol and 20% glycerol solutions. Brains and spinal cords were blocked in the coronal plane. The entire spinal cord was harvested and blocked from one dorsal root entry zone to the next, beginning at the first spinal cord segment through the cauda equina. Blocks were frozen at −80°C until used. Serial coronal sections through the primary motor cortex and the spinal cord were cut on a freezing microtome set at a thickness of 40 μm. For detection of BDA labelling, every 8th section was processed using the avidin–biotin amplification method with peroxide as a substrate. Briefly, sections were washed in 0.1 M Tris-buffered saline (TBS; pH 7.4) three times for 10 min. Incubation with 0.6% hydrogen peroxide in TBS for 30 min reduced the activity of endogenous peroxidases. Sections were rinsed two more times in TBS and then incubated at 4°C overnight in an avidin–biotin–peroxidase complex solution (Vectastain ABC elite kit, Vector Laboratories, CA; 1:500 dilution). After several rinses in TBS, the brain or spinal cord sections were reacted for 10 min in diaminobenzidine with $NiCl_2$ intensification. Following three rinses in TBS, sections were mounted on gelatin-coated slides, air dried, dehydrated, cleared, and coverslipped. Every 8th section was stained for Nissl. Brains also were sectioned in the coronal plane to verify location of BDA cortical injections on Nissl and BDA-labelled sections.

Assessment of lesion completeness

On the lesioned side of the spinal cord, BDA-labelled axons at the L1 level (distal to the lesion) were quantified and compared to numbers of BDA-labelled axons rostral to the lesion (at the T9 level in the dorsolateral fasciculus of five monkeys, and at the T2 level in monkey #2; see below and Table 1). Axon numbers were quantified at 100× magnification using a 10 × 10 counting grid mounted in the microscope ocular, focusing through the plane of section to verify the identity of each object. All BDA-labelled objects of linear profile in the region of interest, i.e. the dorsolateral funiculus ipsilateral to the lesion, were counted. The mean number of axons per section at each level then was calculated. Three sections spaced 320 μm apart at each level were examined (total of six sections per animal). The ratio of distal:rostral axons defined lesion completeness. In monkey #1, BDA tracing was performed, but transport time was inadequate for visualization of BDA-labelled axons. In this monkey, lesion completeness, therefore, was defined on serial Nissl-stained sections. The region of the dorsolateral tract was outlined in a Nissl-stained section 0.5 mm rostral to the lesion site by comparison to the five other BDA-traced subjects in this study. This traced region then was superimposed on the coronal spinal cord section containing the largest area of tissue lesion in the dorsolateral tract. The amount of spared tissue in this monkey was compared to the area of the intact dorsolateral CST to generate a proportion of lesion estimate. Mean lesion extent was calculated for each monkey.

Data collection

After 2–3 weeks of recovery following the EMG implantations, whole body movements and EMG activity (monkeys #1 and #2) were recorded during treadmill locomotion and the foot grasping task under the same experimental conditions as during the training procedure. At the end of the control recordings, the monkeys were subjected to the spinal cord lesion surgery (see above). Post-lesion recordings were started 1 week after surgery (POST-1). Subsequent recordings were done 2 (POST-2), 6 (POST-6) and 12 (POST-12) weeks post-lesion in three monkeys for treadmill locomotion, and 2 (POST-2), 4 (POST-4), 6 (POST-6) and 12 (POST-12) weeks post-lesion in all six monkeys for the grasping task. The methods and procedures used in the present study have been detailed previously (Courtine *et al.*, 2005).

Kinematics

Video recordings (60 Hz) were made using one camera (Panasonic System Camera, WV D5100; Panasonic AG1280P Panasonic, Cypress, CA) oriented perpendicular to the direction of the locomotion. Reflective markers were attached to the shaved skin ipsilateral to the lesion overlying the following body landmarks: for the HL, the greater trochanter (GT), the knee joint (K), the malleolus (M), the 5th metatarsal (MT) and the outside tip (T) of the fifth digit; for the forelimb (FL), the head of the humerus (H), the elbow joint (E), the distal head of the ulna (U), the metacarpo-phalangeal (MCP) joint, and the outside tip of the third digit (D) (see Fig. 3). The body was modelled as an interconnected chain of rigid segments: GT–K for the thigh; K–M for the shank; M–MT for the foot; MT–T for the fifth digit; GT–H for the trunk; H–E for the arm; E–U for the forearm; U–MCP for the hand; MCP–D for the third digit. In addition, the limb axis was defined as the virtual line connecting the hip to the MT joint, and the shoulder to the MCP joint for the HL and FL, respectively.

EMG

Two telemeters (Model T-47, Konigsberg Instruments, Pasadena, CA, USA, bandpass 5–750 kHz) were attached to the EMG skin button and placed in two pouches on the back of the monkey's jacket. The telemeters weighed ~150 g and did not appear to interfere with the performance of the locomotor task. Output from the telemetry receiver was recorded at 2 kHz on FM tape (TEAC Model XR-510, TEAC, Montebello, CA, USA). A Society of Motion Picture and Television Engineers (SMPTE) time code generator (model F30, Fast Forward Video, Irvine, CA, USA) was used to synchronize video frames with the EMG signals recorded on FM tape.

Data processing

Kinematics

(x, y) coordinates of each marker were used to reconstruct the trajectory of the limb and to calculate joint angles at the hip, knee, ankle, and MT joints. The same convention as in cat was used, i.e. flexion and MT plantarflexion were defined as a decrease in the measured angle. Furthermore, the angle of each segment with respect to the direction of gravity (i.e. thigh, shank, foot and toe elevation angles) in the sagittal plane was computed since there is evidence that those angles may be more relevant than joint angles for the sensory (Poppele and Bosco, 2003) and motor (Courtine and Schieppati, 2004) neural control systems. Elevation angles were computed from the displacement of distal and proximal markers attached to each segment, and defined positive in the forward direction, i.e. when the distal marker crossed the vertical line passing through the proximal marker (Courtine and Schieppati, 2004).

Spatial and temporal features of the gait pattern

A gait cycle was defined as the time interval between two successive paw contacts of one limb. Successive paw contacts were visually defined by the investigators with an accuracy of ±1 video frame. Ten successive, consistent HL and FL gait cycles or more were typically recorded from each animal at each discrete treadmill speed and for each walking session. Lesion-induced locomotor deficits, however, prevented us from collecting data at the higher treadmill speeds (1.34 and 1.79 m/s) during the initial 2 weeks post-lesion. The onsets of the swing phases for the limbs ipsilateral to the video recordings were set at the zero crossings of the rate of change of the elevation angle of the limb axis, i.e. at the onset of forward oscillation. Swing phase onsets for the contralateral limbs were determined from the video recordings. The unilateral lesion of the CST resulted in a dragging of the hindpaw ipsilateral to the lesion. The extent of the paw drag during each gait cycle was considered as the time during which the paw was in contact with the treadmill belt expressed as a percentage of the swing duration (forward HL movement). Cycle duration, stride length and stance and swing durations were determined from the video recordings. The mean body speed was computed during each cycle as the stride length divided by the cycle duration: mean body speed per cycle differed from treadmill speed owing to longitudinal displacements of the animal along the treadmill belt, particularly post-lesion. Footfall patterns were used to compute the coupling between the HLs and between the HL and FL.

Limb endpoint

We analysed the trajectory of the distal-most marker (T) of the foot, i.e. HL endpoint, relative to a fixed extrinsic frame attached to the treadmill. Therefore, the HL endpoint trajectory appeared as video

recorded except that the position of the marker (T) was corrected by subtracting the mean horizontal GT position cycle-by-cycle to account for possible drifting of the monkey along the treadmill during the recording session. The extent of backward and forward HL oscillation with respect to the hip was computed as the minimal and maximal value of the T-to-GT marker distance over the time interval of each gait cycle.

Inter-segmental coordination

We used principal component (PC) analysis to quantify the spatio-temporal structure of the inter-segmental coordination among body segments (Courtine and Schieppati, 2004). For each set of trial data, the analysis was performed on elevation angles ($n = 4$) of the HL ipsilateral to the lesion. The number of components required to account for data variance was used to provide insight into the complexity of the spatio-temporal structure of the underlying inter-segmental coordination pattern.

EMG

Raw EMG signals were band-pass filtered (30 Hz to 1 kHz), rectified, time-interpolated over a time base with 1000 points for individual gait cycles, and averaged. Onsets and ends of EMG burst activity of each muscle recorded during each gait cycle were identified (Courtine *et al.*, 2005). Cycle period was calculated as the time between the onset points of successive bursts of EMG activity in the Sol muscle. Burst duration and amplitude were calculated as the time and the integral of the muscle envelope, respectively, between the onset and the end of an individual burst. The EMG amplitude of each burst was normalized to the mean burst amplitude of the same muscle when walking at 0.45 m/s, i.e. the slowest treadmill speed.

Foot grasping task

Performance of monkeys in the foot grasping task was quantified from the video recordings. A successful trial was defined as the ability to pick the item up from the presenting platform and transport it to the mouth. Success/failure rate was computed. Activity of selected muscles was analysed in the two monkeys implanted with chronic EMG electrodes. EMG signals were processed using the same procedures as for the locomotor task. Onsets and ends of EMG burst activity were identified visually for each trial. The amplitude of muscle activity was calculated as the mean value of the rectified and filtered EMG signal between the onset and the end of an individual burst.

Statistical analysis

For each monkey, we calculated the mean values and standard deviations of the different parameters over all trials for each experimental condition. Repeated-measures ANOVAs were used to test the effect of the different conditions on the experimental parameters. The factors examined were the testing session (PRE, POST-1, POST-2, POST-4, POST-6 and POST-12) and the body side (ipsilateral and contralateral to the lesion). A P-value <0.05 was considered significant. *Post hoc* differences were assessed by the Newman–Keuls test. Unpaired t-tests were used to assess any differences between pre- and post-lesion data within each animal. Linear regression analyses were performed to determine the relationships between variables. Differences between the slopes of the linear regressions were determined using unpaired t-tests. The software package Statistica® was used for these analyses.

Results

Verification of lesion location and extent

Lesion placement was evaluated by examination of serial Nissl-stained sections through and beyond the lesion site, comparing the lesion location to known sites of appearance of the lumbar enlargement and the nucleus dorsalis of Clarke. Lesions were located at the T10 level in five subjects, and at the T3 level in one subject (monkey #2) (see Table 1). BDA injections into the motor cortex contralateral to the lesion side were performed 3 weeks prior to sacrifice and were accurately targeted in 6 of 6 monkeys. The pattern of BDA labelling in the spinal cord was similar in the five monkeys that underwent successful tracing (see Methods). As previously observed (Lacroix *et al.*, 2004), the greatest density of axonal labelling was present in dorsolateral white matter contralateral to the side of cortical BDA injection (contralateral dorsal CST). In addition, ~10% of the corticospinal axons descend in the ipsilateral dorsolateral CST, and these axons were well visualized in all five monkeys. Minor labelling also was present in the ipsilateral ventromedial white matter (ventral CST). Axonal labelling abruptly terminated at the lesion site, with evident retraction bulbs. Lesion completeness was assessed by measuring the relative proportion of dorsolateral CST axons detectable below compared to above the lesion site (Fig. 2) in the five successfully traced monkeys. The numbers of counted axons one segment caudal and one segment rostral to the lesion as well as the lesion completeness are reported in Table 1 for each animal. In monkey #1, lesion completeness was estimated by measuring lesion extent in the dorsolateral region of the spinal cord. The extent of dorsolateral tract corticospinal fibre interruption ranged from 35 to 99% (Fig. 1). The effects of possible lesions of non-CST pathways are considered in the Discussion section.

Post-lesion changes in locomotion kinematics

All three monkeys tested for locomotor ability (monkeys #1, #2 and #3) were able to walk unaided quadrupedally for extended periods on the treadmill as early as 1 week post-lesion. The two animals most affected by the lesion (monkeys #2 and #3), however, could not locomote at speeds >0.89 m/s during the initial 2–3 weeks post-lesion. The most obvious locomotor deficit was the dragging of the hindpaw ipsilateral to the lesion along the treadmill belt during the swing phase (paw drag). As illustrated in Fig. 3A, paw drag was observed in monkeys #2 and #3, and the extent of the paw drag was larger at 0.45 than 0.89 m/s (data not shown, t-test, $P < 0.05$ for both animals). Monkey #1 also showed a dragging of the hindpaw when stepping overground, but not on the treadmill (light touch only). Paw drag was reflected in the increased plantarflexion of the metatarso-phalangeal (MTP) joint and the reduced ankle dorsiflexion during the swing phase of gait (Fig. 3B). Note that the three monkeys exhibited similar directional joint angle changes during treadmill stepping post-lesion, although the amplitude of these changes varied across

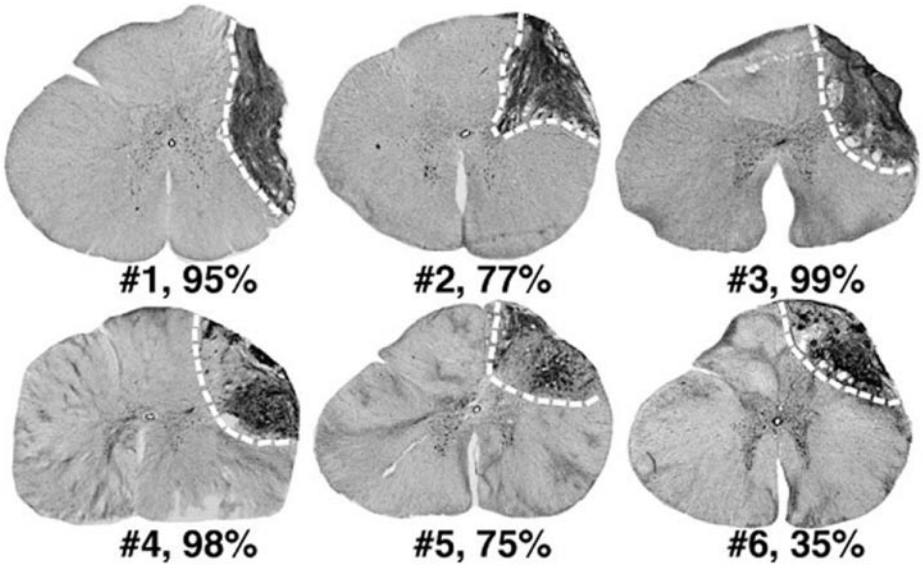

Fig. 1 Nissl stain demonstrating thoracic CST lesion in monkey. White dashed line indicates lesion margins; percentage indicates proportional interruption of CST on lesioned side (see text). Transverse sections have been flipped when needed to show the lesion on the right aspect of the spinal cord (see Table 1 for lesion side).

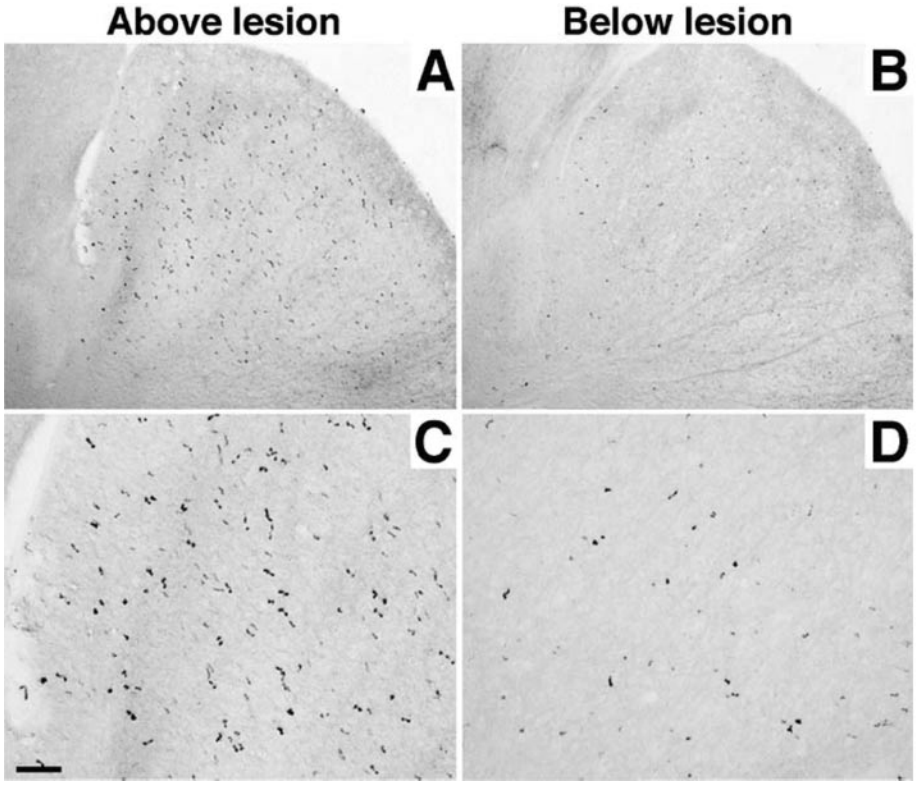

Fig. 2 BDA-labelled CST. Low- (**A**, **B**) and high-magnification (**C**, **D**) of dorsolateral CST above (**A**, **C**) and below (**B**, **D**) the lesion site. Examples are from monkey # 5 at T8 (**A**, **C**) and L1 (**B**, **D**) spinal levels. Scale bar: 225 μm in **A**, **B**; 85 μm in **C**, **D**.

the animals depending upon the extent of the paw drag. Compared to pre-lesion values, the amplitude of the hip angle increased at one week post-lesion (ANOVA, $P < 0.01$ for both conditions of treadmill speeds). In contrast to the hip joint, the knee joint had a reduced range of motion (ANOVA, $P < 0.05$), and was more flexed throughout most of the step cycle at 1 week post-lesion than pre-lesion. Furthermore, the hip reached its most extended position earlier (ANOVA,

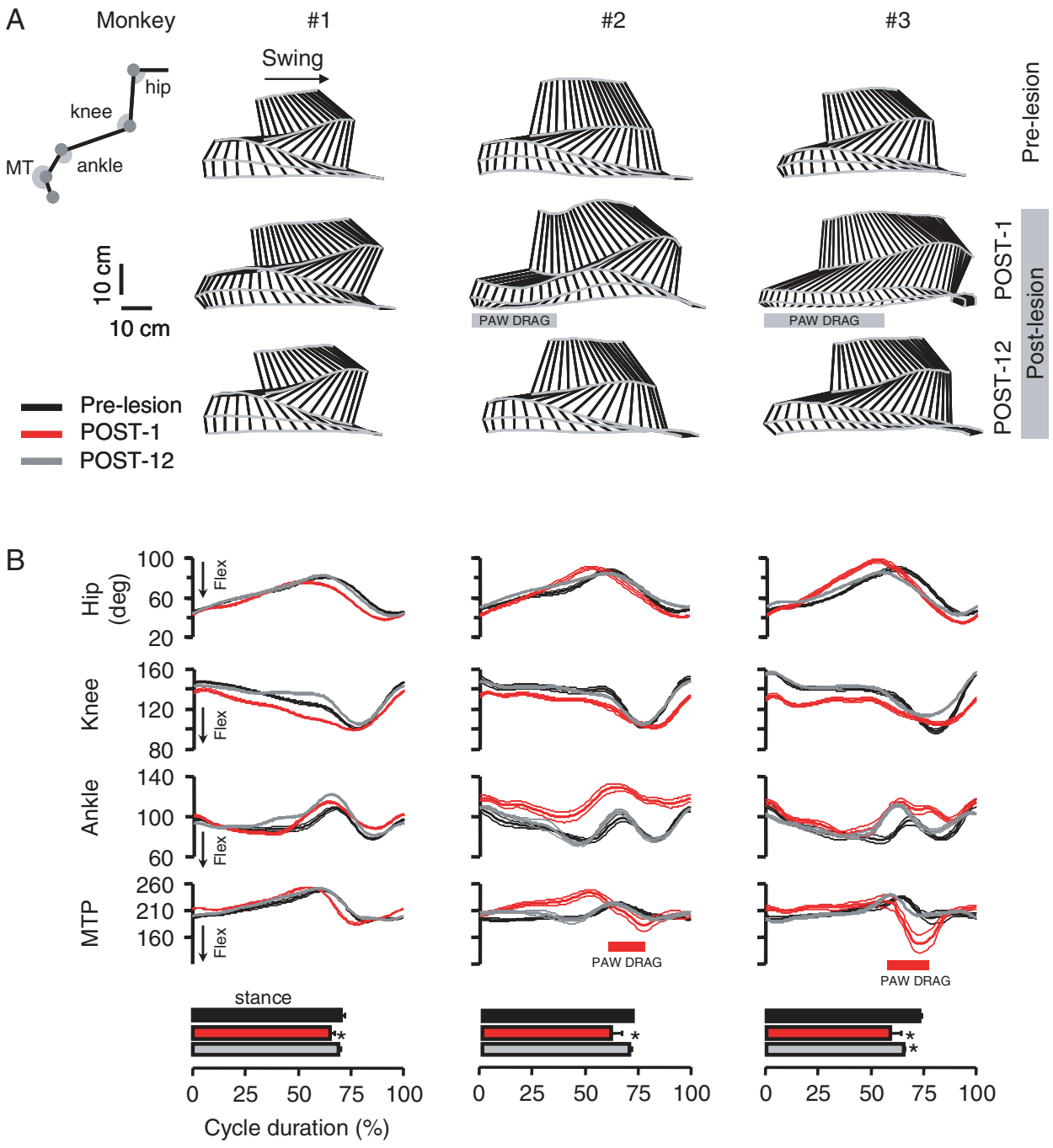

Fig. 3 (**A**) Representative stick diagram decompositions of HL movements for the side ipsilateral to the CST lesion during the swing phase while stepping quadrupedally on the treadmill at 0.45 m/s before, and 1 and 12 weeks after the lesion in the three monkeys tested. Horizontal bars at 1 week post-lesion indicate the period of paw drag for monkeys #2 and #3. There was no paw drag in monkey #1. (**B**) Mean (SD) waveforms of each joint angle for the HL ipsilateral to the CST lesion recorded at a treadmill speed of 0.45 m/s before (Pre-lesion) and 1 (POST-1) and 12 (POST-12) weeks after the lesion are plotted versus the normalized gait cycle duration for each monkey. The horizontal bars at the bottom indicate the mean (SD) value of the stance phase duration. Asterisk indicates significant difference between pre- and post-lesion values. The convention used to compute the joint angles is shown in the inset at the upper left.

$P < 0.001$) and the knee flexed for a longer period (ANOVA, $P < 0.001$) after than before the lesion. These changes resulted in a marked modification of the temporal coupling between the hip and knee joints (ANOVA, $P < 0.001$) that probably contributed to the dragging of the foot during the swing phase post-lesion. At 1 week post-lesion, all monkeys showed increased plantarflexion at the ankle and increased flexion at the MTP joint during the stance phase. There was no paw drag in monkey #2 by the second week post-lesion, but paw drag occurred occasionally in monkey #3 up to

3 weeks post-lesion. Paw drag never occurred when the animals were tested 12 weeks post-lesion. Consequently, the locomotion kinematics recorded pre-lesion and 12 weeks post-lesion were comparable, although some discrepancies, in particular at the ankle (Fig. 3B), were still observable. Monkeys #4 and #5 showed similar locomotor deficits including paw drag and gait instability. Impairment of walking ability, if any, was very limited in monkey #6. Kinematic analysis could not be performed in these latter three animals.

Lesion-induced changes in the timing and magnitude of HL joint excursions substantially modified the path of the limb endpoint (tip of the toe). The typical path covered by the endpoint of the HL ipsilateral to the lesion during one complete gait cycle (stance and swing) before the lesion, and 1 and 12 weeks after the lesion are depicted in Fig. 4A. Changes in the limb endpoint path at 1 week post-lesion typically involved a larger hip-to-endpoint horizontal distance at the end of stance (ANOVA, $P < 0.01$; *post hoc*, $P < 0.05$ for POST-1 and POST-2) (Fig. 4B), a drag of the endpoint along the treadmill belt during the early part of the swing phase (Fig. 4A), and a marked upward movement late in swing (Fig. 4A). Interestingly, the HL endpoint path before and 12 weeks post-lesion were similar in shape. Nevertheless, the limb endpoint still reached a more backward position at the end of stance in both monkeys #2 and #3 (*t*-test, $P < 0.05$; significant only for these two monkeys).

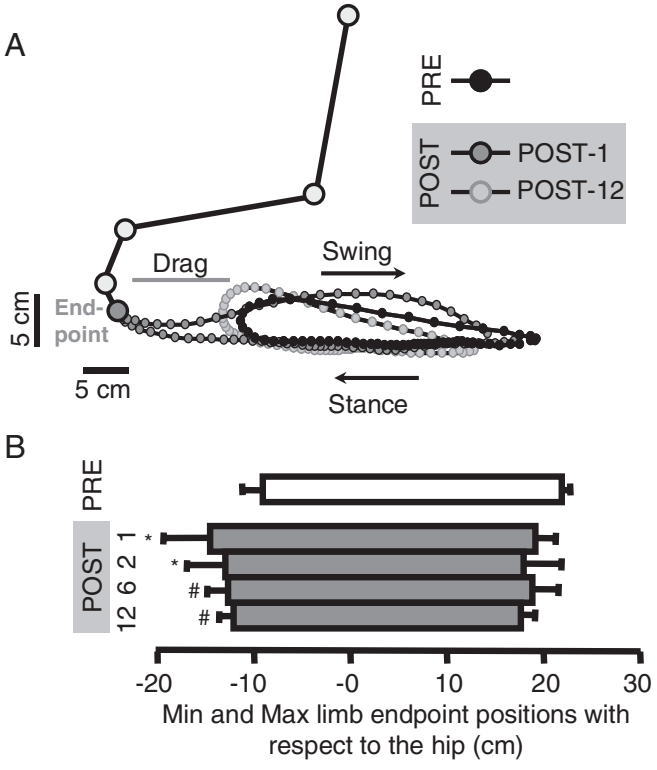

Fig. 4 (**A**) Typical path for the endpoint (tip of the toe) of the HL ipsilateral to the CST lesion during a complete gait cycle for monkey #2 at a treadmill speed of 0.45 m/s before the lesion, and 1 and 12 weeks after the lesion. (**B**) Mean (SD) values for the minimal (left) and maximal (right) positions reached by the HL endpoint with respect to the hip (horizontal distance) during each gait cycle at each time point tested. Asterisk indicates significant difference between pre- and post-lesion values for all monkeys (ANOVA); hash indicates significant differences between pre- and post-lesion values only for monkey #2 and #3 (*t*-test).

Changes in inter-segmental coordination

Elevation angles, i.e. the angle with respect to the direction of gravity, were used to investigate inter-segmental coordination patterns since there is evidence that both sensory (Poppele and Bosco, 2003) and motor (Lacquaniti *et al.*, 2002; Courtine and Schieppati, 2004) neural systems may preferentially control the displacement of the limbs with respect to the direction of gravity than the joint angles *per se*. In Fig. 5A, the mean (all trials at 0.45 m/s) elevation angles for the thigh, shank, foot and toe segments are plotted versus the normalized gait cycle duration for each time point tested for monkeys #2 (left) and #3 (right). These plots illustrate that the spatial and temporal features of the HL segment angular trajectories were affected the most at the early time points and then progressively returned toward normality. Nevertheless, substantial discrepancies in the HL kinematics between pre- and post-lesion recordings persisted throughout the recovery period, and significant differences were observed up to 12 weeks post-lesion in monkeys #2 and #3 (black versus grey traces in Fig. 5A). PC analysis was used to evaluate the effects of the CST lesion on inter-segmental coordination. The variance attributable to the first PC quantified the degree of linear co-variation in the coupling between thigh, shank, foot, and toe oscillations (Courtine and Schieppati, 2004). In normal walking conditions, the first PC explained >85% of the total data variance (Fig. 5B). A decrease (*t*-test, $P < 0.05$) in the variance due to PC_1 was observed at 1 week post-lesion in all three monkeys. These values then converged toward the pre-lesion baseline over time, and did not differ statistically from pre-lesion data at POST-6 or POST-12 except for monkey #2.

Changes in the spatial and temporal structure of gait and associated EMG activity

The three monkeys for which kinematic data were available showed a significant change in step cycle duration of the HL ipsilateral to the CST lesion post-lesion (ANOVA, $P < 0.001$). Mean cycle durations were longer (*post hoc*, $P < 0.05$) at treadmill speeds of 0.45 and 0.89 m/s at 1 and 2 weeks post-lesion (Fig. 6A) and were similar to pre-lesion values thereafter. The same changes were detected in the HL contralateral to the lesion (ANOVA, $P < 0.001$), i.e. both HLs progressed at similar frequency pre- and post-lesion ($P = 0.9$). Mean FL cycle durations could slightly increase (#1), decrease (#2), or remain unchanged (#3) (overall mean unchanged, data not shown). In all instances, however, the mean cycle duration was longer for the HL compared to the FL at week 1 post-lesion (ANOVA, $P < 0.05$). In Fig. 6B, the cycle durations

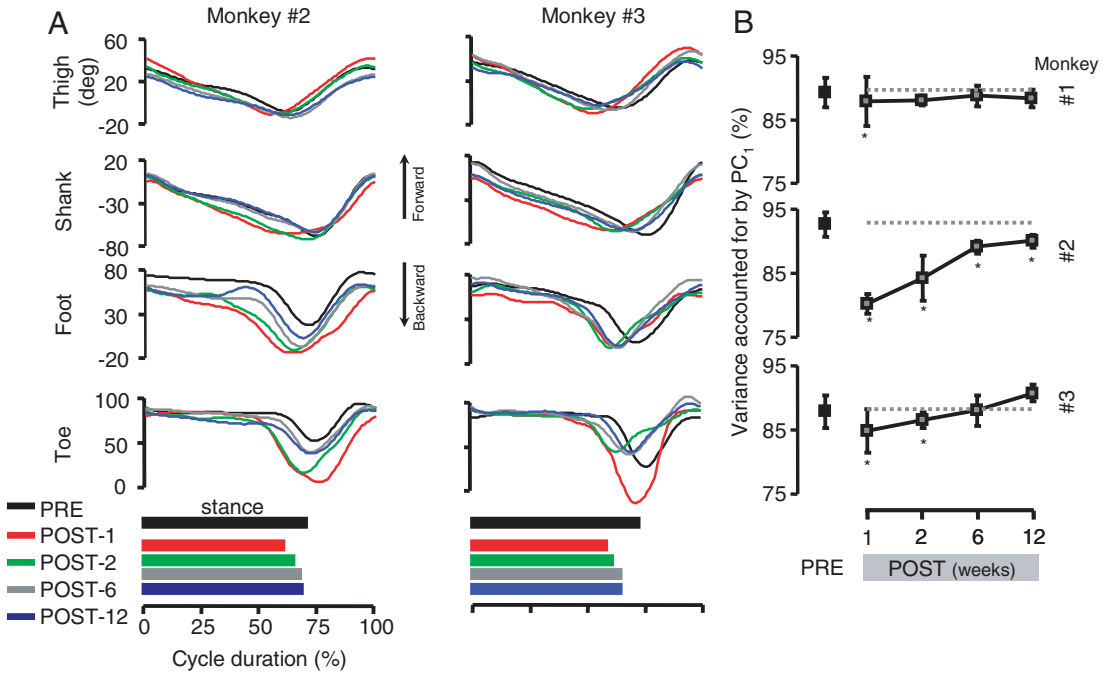

Fig. 5 (**A**) Mean waveforms of each elevation angle, i.e. the angle with respect to the direction of gravity, of the HL ipsilateral to the CST lesion for all gait cycles performed by monkey #2 (left) and #3 (right) at 0.45 m/s for each day of testing. The different colours differentiate the days of testing. The horizontal bars at the bottom indicate the mean value of the stance duration for each day of testing. (**B**) Mean (SD) values of the variance accounted for by the first PC for each monkey for each day of testing. Asterisk indicates significant difference between pre- and post-lesion values for each monkey.

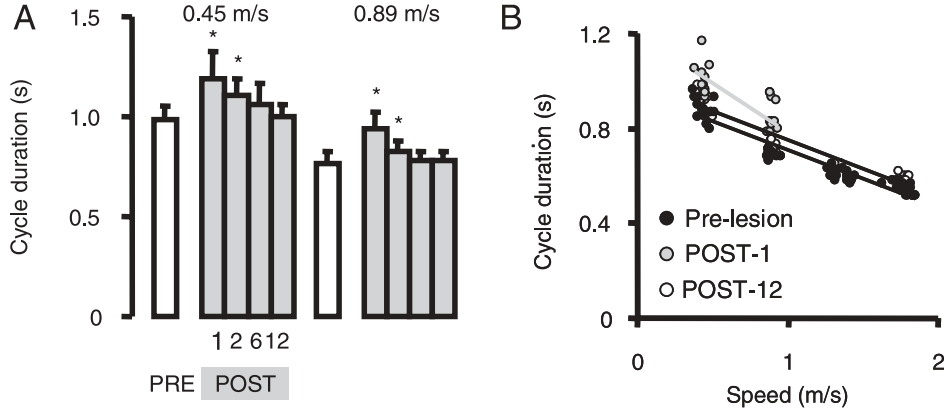

Fig. 6 (**A**) Mean (SD) values for cycle duration for the HL ipsilateral to the lesion at two treadmill speeds pre-lesion and 1, 2, 6 and 12 weeks post-lesion (pooled data from three monkeys). Asterisk indicates significant difference between pre- and post-lesion values. (**B**) Relationship between mean body speed and cycle duration for all gait cycles recorded from the HL ipsilateral to the CST lesion before and 12 weeks after the lesion for monkey #1. All correlations were significant ($P < 0.001$).

for all individual steps recorded for the HL ipsilateral to the lesion for monkey #1 are plotted versus the mean body speed. The increase in HL cycle duration post-lesion resulted in an increase ($P < 0.001$) in the slope of the speed-to-cycle duration relationship at 1 week post-lesion compared to pre-lesion. No significant differences between pre- and post-lesion relationships were observed at the end of the recovery period (Fig. 6B). Similar changes were observed in all three monkeys tested.

Unilateral interruption of the CST projections produced bilateral, side-dependent changes in HL stance duration in all three monkeys. Compared to pre-lesion values, the mean relative (% of cycle duration) stance duration of the HL ipsilateral to the lesion was decreased (ANOVA, $P = 0.001$) at 1, 2 and 6 weeks post-lesion, and that of the HL contralateral to the lesion was increased (ANOVA, $P < 0.01$) at 1 week post-lesion (Fig. 7A). The slope of the relationship between the cycle duration and stance duration for the HL contralateral

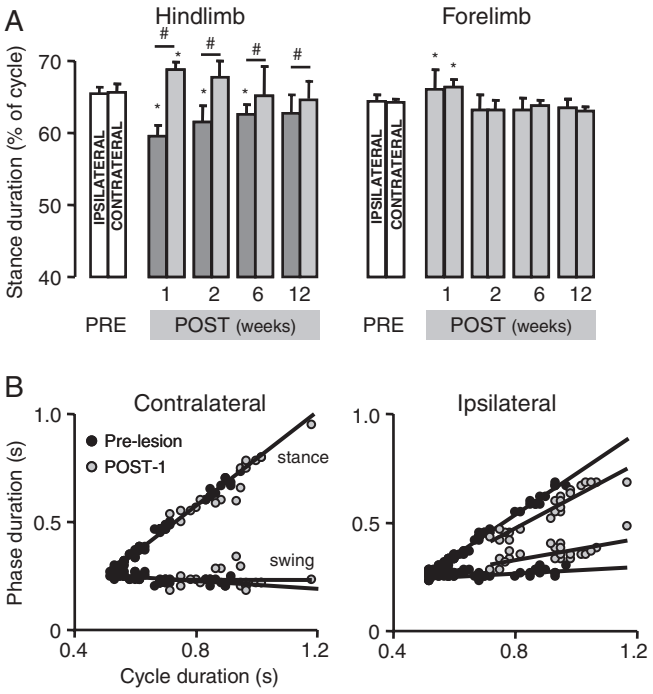

Fig. 7 (**A**) Mean (SD) values for stance duration from the HL and FL ipsilateral and contralateral to the lesion at a treadmill speed of 0.89 m/s are shown for pre-lesion and 1, 2, 6 and 12 weeks post-lesion recordings (pooled data from three monkeys). Asterisk, hash indicates significant difference between pre- and post-lesion values, and between ipsilateral and contralateral limbs, respectively. (**B**) Relationship between cycle duration and stance/swing duration for the HL on the ipsilateral and contralateral sides to the CST lesion ($P < 0.01$ for all correlations, see Table 3). All gait cycles pre-lesion and 1 week after the lesion are displayed for monkey #1.

Table 3 Slope and correlation coefficient (*r* value) of the relationship between cycle duration and stance duration of gait (upper part) or muscle burst duration (lower part) computed before the CST lesion and 1 week after the lesion for the hindlimb (HL) ipsilateral and contralateral to the lesion side for each monkey

Monkey	Ipsilateral HL		Contralateral HL	
	Pre	Post-1	Pre	Post-1
Cycle period/stance duration				
Slope				
#1	0.95	0.76*	1.02	0.99
#2	0.85	0.52*	0.96	0.92
#3	0.90	0.46*	0.84	0.86
r value				
#1	0.99	0.89*	0.99	0.98
#2	0.99	0.95*	0.99	0.92*
#3	0.99	0.84*	0.99	0.94*
Cycle period/EMG burst duration				
Slope #1				
Sol	0.87	0.58*	0.80	0.91*
MG	0.69	0.39*	0.86	0.85
VL	0.81	0.56*	0.70	0.88*
TA	−0.08	0.30*	−0.06	−0.09
Slope #2				
Sol	0.73	0.53*		
MG	0.7	0.53*	0.68	0.78*
FHL	0.81	0.51*		
FDL	0.94	0.47*		

Asterisks indicate significant difference between pre- and post-lesion (1 week) values.

to the lesion was not significantly changed post-lesion (Table 3 and Fig. 7B, left). In contrast, the slope of this relationship for the HL ipsilateral to the lesion was decreased in all three monkeys tested ($P < 0.05$, Table 3 and Fig. 7B, right). The slope of the relationship between the cycle duration and swing duration was conversely increased (Fig. 7B, right). In addition, correlation coefficients were weaker for post- versus pre-lesion data for both HLs ($P < 0.001$ for all monkeys and limbs except the contralateral HL of monkey #1). Stance duration remained longer (*post hoc*, $P < 0.05$) for the HL contralateral versus the HL ipsilateral to the lesion at all time points post-lesion (Fig. 7A). Significant changes in the relative stance duration of both FL also were detected (ANOVA, $P < 0.05$). The mean relative duration of the stance phase was increased (*post hoc*, $P < 0.01$) in the FL ipsilateral and contralateral to the lesion at 1 week post-lesion (Fig. 7A).

These changes in the intrinsic timing of gait were reflected in the activation patterns of the HL muscles (Fig. 8). Before the lesion, the extensor muscles (Sol, MG, FHL, and VL) were activated during the stance phase, whereas the flexor muscle (TA) was recruited during the swing phase of gait (Fig. 8). Accordingly, there were close relationships between the duration of the cycle period and the duration of the EMG burst, for both extensor and flexor muscles (data not shown). The side-dependent changes in stance duration resulted in a decrease in the extensor EMG burst durations on the ipsilateral and an increase on the contralateral side to the lesion (*t*-test, $P < 0.001$; Fig. 8). Flexor burst duration increased on the ipsilateral and decreased on the contralateral side (*t*-test, all post-lesion time points, $P < 0.001$; Fig. 8). Consequently, there were differences in the slopes of the cycle duration-to-burst duration relationships between the ipsilateral and contralateral HL extensor muscles (all comparisons, $P < 0.05$; Table 3). Compared to the pre-lesion baseline, the slope of the relationship between cycle duration and TA burst duration did not change significantly on the contralateral side, but increased on the ipsilateral side ($P < 0.001$; Table 3). This observation is consistent with the modification of the relationship between the cycle duration and the swing phase duration (Fig. 7B and Table 3). Interestingly, after the lesion the recruitment of the flexor digitorum longus (FDL) was not restricted to the second half of the stance phase as seen under normal walking conditions; instead the FDL was activated throughout the support period concomitantly with the leg extensors at all time points (Fig. 8).

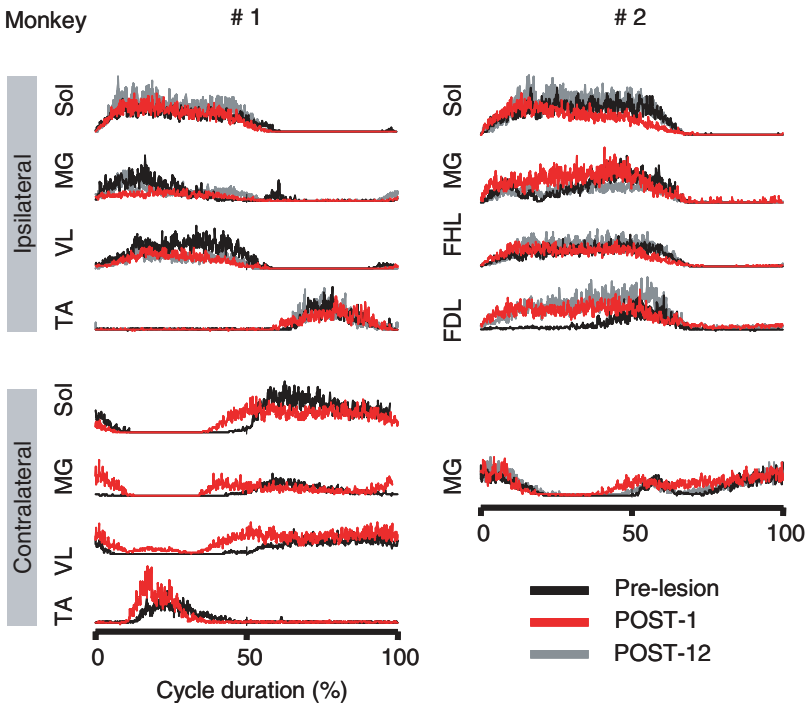

Fig. 8 Mean (n = 20 steps) integrated EMG activity of selected ipsilateral and contralateral HL muscles recorded from monkey #1 and #2 before the lesion, and 1 and 12 weeks after the lesion is shown. Waveforms are aligned with the onset of the Sol EMG burst from the HL ipsilateral to the lesion. Muscles contralateral to the lesion could not be recorded in monkey #1 during POST-12 testing.

Changes in the amplitude of EMG activity

Some similarities and differences were observed in lesion-induced modifications of the EMG burst amplitude between the two monkeys (Figs 8 and 9). For example, the Sol and MG muscles ipsilateral to the lesion showed opposite changes post-lesion in monkeys #1 versus #2. However, the EMG burst amplitude of the Sol muscle on the ipsilateral side for both monkeys was significantly higher at POST-6 and POST-12 than pre-lesion. Likewise, the MG EMG amplitude for both monkeys returned to the pre-lesion baseline at POST-6 and POST-12. In addition, there was an increase in the EMG burst integral of the MG contralateral to the lesion in both monkeys during the initial 2 weeks post-lesion (t-test, $P < 0.001$). Changes in the amplitude of extensor muscle activation were variable in the muscles ipsilateral to the lesion, i.e. decreased or increased (Figs 8 and 9), whereas the level of activity generally increased in the contralateral muscles (Figs 8 and 9). The recruitment of the ipsilateral FDL muscle, which was active during the entire stance duration (see above, Fig. 8), was associated with a dramatic increase in its integrated EMG activity at all time points post-lesion (t-test, $P < 0.001$; Fig. 9). Furthermore, the integral of the EMG burst for the ipsilateral flexor hallucis longus (FHL) muscle progressively increased over the post-lesion testing period compared to the pre-lesion baseline (Figs 8 and 9). The tibialis anterior (TA) muscle burst amplitude was unchanged on the ipsilateral side post-lesion (Fig. 9), most likely as a consequence of the increased burst duration (Fig. 8). In turn, the contralateral TA muscle was more heavily recruited post- compared to pre-lesion (t-test, $P < 0.001$; Fig. 9), consistent with the rapid dorsiflexion of the foot during a shortened swing phase (see above).

Changes in inter-limb coordination

All of these modifications in the spatial and temporal structure of the gait pattern affected inter-limb coordination. Fig. 10A shows the gait diagram reconstructed from a typical trial at 0.45 m/s for monkeys #2 and #3 performed before the lesion, and at 1 (POST-1) and 12 (POST-12) weeks post-lesion. Each box indicates the time during which a given limb is in contact with the ground (stance phase), and empty spaces correspond to the swing phase. During the pre-lesion recordings, monkeys #1 and #2 displayed a well-organized diagonal footfall pattern in which the footfall of a FL roughly coincided with that of the contralateral HL (Fig. 10A, left). Monkey #3 used a lateral footfall pattern, i.e. the footfall of a FL occurred just after the footfall of the ipsilateral HL (Fig. 10A, right). By 1 week post-lesion, the coupling between the HL and FL was significantly disrupted: the different frequencies in HL and FL stepping resulted in a gradual phase deviation between the HL and FL. As a consequence, no clear relationship could be detected between HL and FL footfalls for monkey #2 (Fig. 10A, left). Although not as dramatic, a progressive drift in the coupling between the HL and FL ipsilateral to the lesion can also be observed

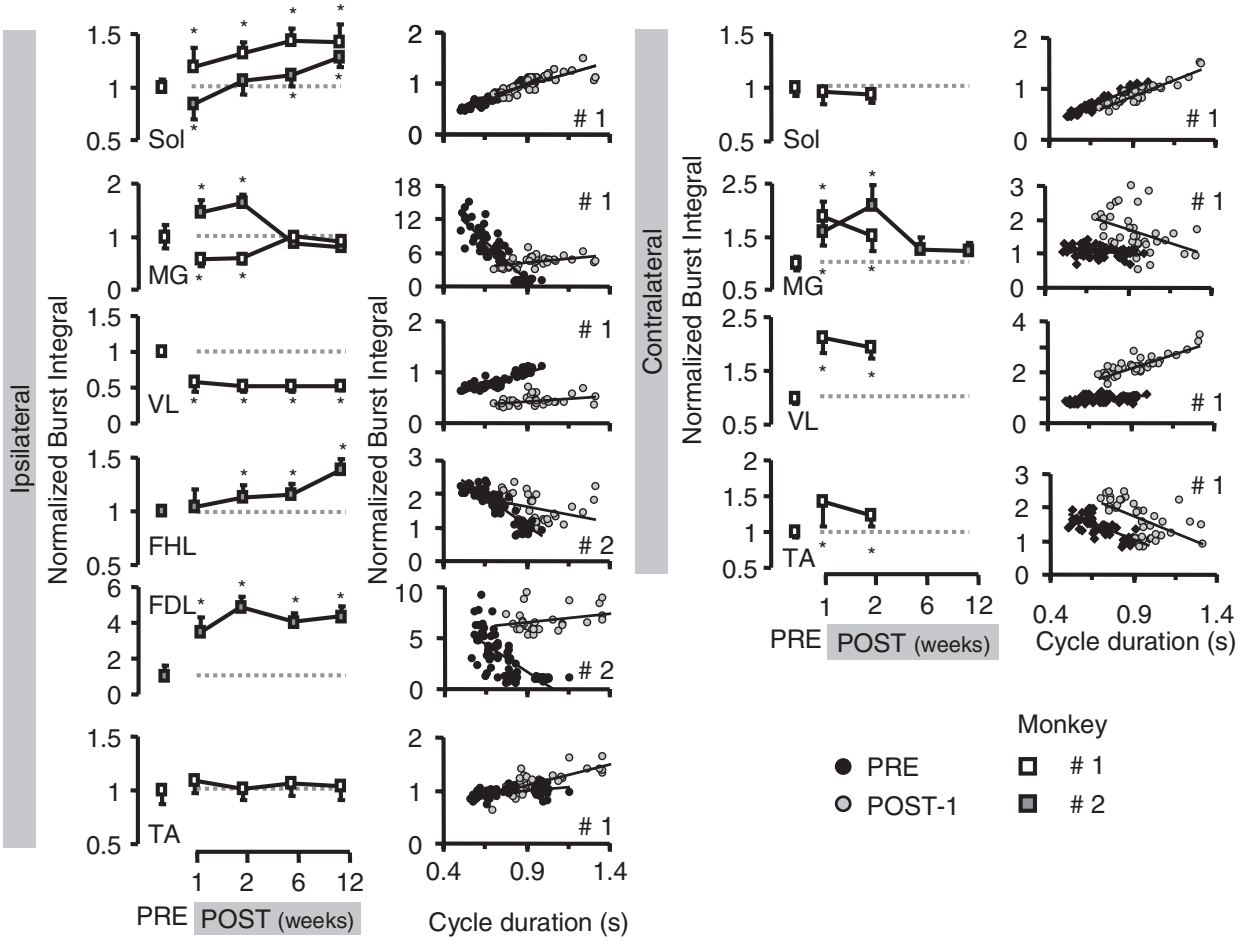

Fig. 9 Mean (SD) values of EMG burst integrals for all recorded muscles from monkey #1 (open squares) and #2 (filled squares) at a treadmill speed of 0.89 m/s on each day of testing. Values are normalized to the pre-lesion baseline (dashed lines) computed as the mean value of muscle activity during pre-lesion locomotion at 0.45 m/s. Contralateral muscles could not be recorded after the second week post-lesion in monkey #1. Asterisk indicates significant difference between pre- and post-lesion values (*t*-test). Relationship between cycle duration and EMG burst integral is also shown for the same muscles for monkeys #1 or #2 (indicated in each plot) pre-lesion and 1 day post-lesion. All correlations were significant ($P < 0.01$, r value range, $0.6 < r < 0.96$).

in monkey #3 (Fig. 10A, right). Variability of the coupling between homolateral limbs was quantified as the coefficient of variation (CV) of the timing between footfalls of the HL and FL ipsilateral to the lesion (Fig. 10B). When the monkeys walked at either treadmill speed tested, the variability of homolateral coupling increased as much as 5–10-fold at the first week post-lesion (ANOVA, $P < 0.001$), remained elevated at 2 weeks post-lesion (ANOVA, $P < 0.05$) and was similar to pre-lesion values thereafter. In addition, the coupling between the left and right HL was consistently modified following the CST lesion (ANOVA, $P < 0.001$). The left and right HLs moved perfectly out of phase before the lesion regardless of the inter-limb coupling pattern (diagonal or lateral), i.e. footfall of the contralateral HL occurred at 50% of the ipsilateral HL cycle duration (Fig. 10C). After the lesion, the contralateral HL systematically anticipated the beginning of its stance phase with respect to that of the ipsilateral HL (*post hoc*, POST-1 and POST-2, $P < 0.01$). Accordingly, the onset and end of the EMG bursts of the extensor and flexor muscles contralateral to the lesion, respectively, occurred relatively earlier post- than pre-lesion (*t*-test, $P < 0.05$; Fig. 8).

General post-lesion changes in foot grasping task

The CST lesion completely abolished (two-way ANOVA, $P < 0.01$; *post hoc*, $P < 0.001$) the ability of four out of the six monkeys to retrieve food items with the foot ipsilateral to the lesion during the first 2 weeks post-lesion (Fig. 11A). Monkey #2 also was impaired significantly, but retrieved a small percent of items as early as 1 week post-lesion (25% success). Most CST axons were spared in monkey #6 (35% lesioned; Fig. 1), and only modest decrease in performance was observed for this animal (67% success; not included in Fig. 11A or the statistical analyses). Accordingly, a significant ($P < 0.001$) relationship was found between CST lesion completeness and the percentage of item retrieval failure at 1 week

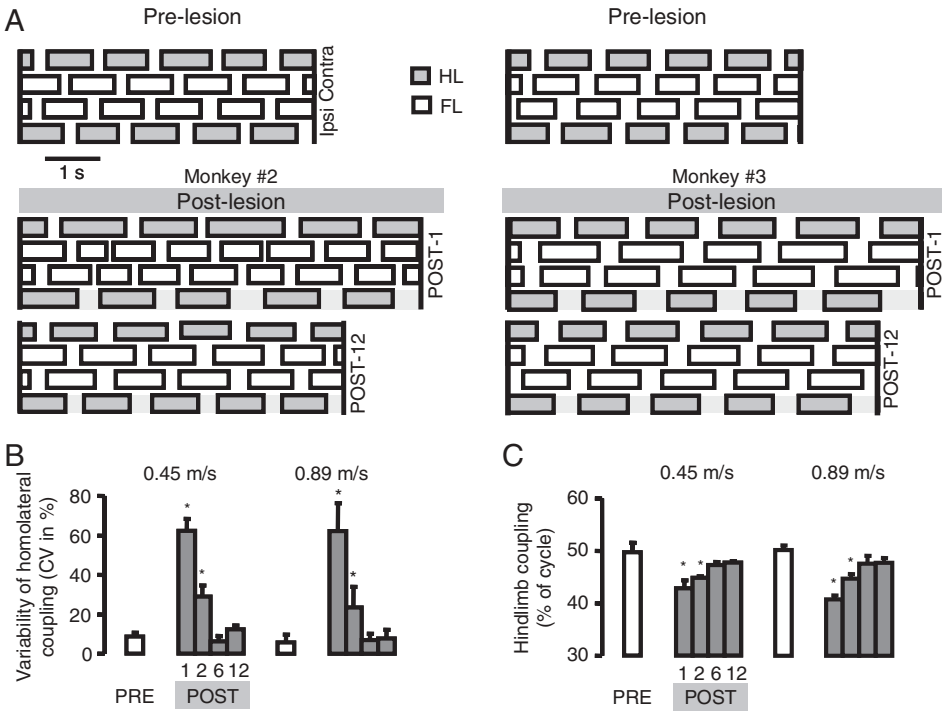

Fig. 10 (**A**) Gait diagrams reconstructed from the displacement of the four limbs during a typical treadmill trial for monkey #2 (left) and #3 (right) at 0.45 m/s before, and 1 and 12 weeks after the CST lesion. Boxes and empty spaces correspond to the stance and swing phases of gait, respectively. Five complete gait cycles of the HL ipsilateral to the lesion are represented in each gait diagram. (**B**) Mean (SD) values of homolateral coupling variability, i.e. coupling between the HL and FL ipsilateral to the lesion, for two treadmill speeds pre-lesion (open bars) and 1, 2, 6 and 12 weeks post-lesion (filled bars) (pooled data from three monkeys). (**C**) Mean (SD) values for the temporal coupling between HL displacements. These values were computed as the time of paw contact of the HL contralateral to the lesion with respect to paw contact of the HL ipsilateral to the lesion expressed as a percentage of the ipsilateral HL cycle duration (pooled data from three monkeys). Asterisk indicates significant difference between pre- and post-lesion values in (**B**) and (**C**).

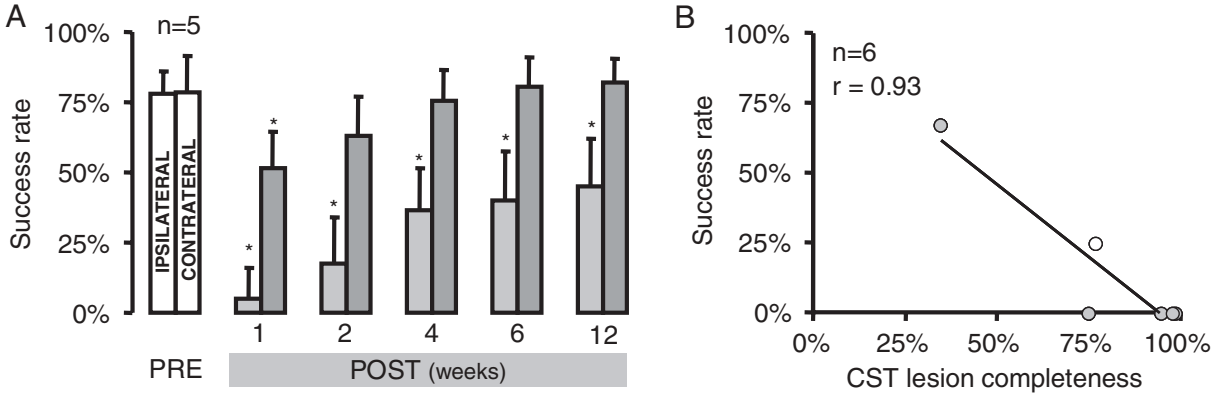

Fig. 11 (**A**) Percent of successful item retrievals with the foot for pre-lesion and 1, 2, 4, 6, and 12 weeks post-lesion testing; all item sizes are pooled ($n = 30$). Data are presented as the average (SD) of the performance for monkeys #1 to #5 (monkey #6 is not included since the lesion was incomplete, see text). The performances of the foot ipsilateral and contralateral to the lesion are reported. Asterisk indicates significant difference between pre- and post-lesion values. (**B**) Relationship between CST lesion completeness (%) and percentage of successful item retrievals for 1 week post-lesion testing ($P < 0.001$). Monkey #2 (T3 lesion) is depicted by the open circle.

post-lesion (Fig. 11B). The ability of the monkeys to retrieve items with the foot ipsilateral to the lesion remained impaired 12 weeks post-lesion compared to the pre-lesion baseline (*post hoc*, $P = 0.02$), although most animals improved their performance over the duration of the recovery period. Near-complete recovery was observed as early as 2 weeks post-lesion in monkey #2. The strategy used during successful retrieval of items, however, differed post- compared to pre-lesion. After the CST lesion, the monkeys did not grasp the item between their great toe and 2nd digit as they did pre-lesion, but instead used the digits as a hook to pick up the item from the platform. The monkeys have been shown to exhibit a similar

strategy to retrieve a food reward with the hand following a pyramidal tract lesion (Lawrence and Kuypers, 1968*a*) or a complete cervical hemisection (Galea and Darian-Smith, 1997*b*). A decrease in foot grasping performance also was observed on the side contralateral to the lesion (two-way ANOVA, $P < 0.01$). *Post hoc* tests revealed a disruption of performance during the first 2 weeks post-lesion compared to pre-lesion (*post hoc*, $P < 0.05$). The item size (small, medium, or large) had no significant effect on the level of performance, although retrieval of smaller items tended ($P = 0.1$) to be more challenging than larger items following the lesion. The absence of statistical significance was partly due to the fact that during some trials the monkeys stuck the raisin to their foot, and transported the raisin to their hand without having to grasp it.

Changes in EMG activity during foot grasping task

Successful execution of the foot grasping task pre-lesion involved a stereotypical sequential activation of flexor and extensor muscles of the ankle (Fig. 12A, left). This included (A) a short burst of the TA muscle to lift the foot off the ground, (B) a prolonged activation of the MG muscle to produce foot plantarflexion and reach the item, (C) a phasic and (D) tonic activation of the TA muscle to generate and maintain, respectively, foot dorsiflexion during transport of the item to the mouth (or hand) and (E) moderate activation of the TA muscle when returning to the resting position (F). The CST lesion completely abolished the ability of the monkey depicted in Fig. 12A (monkey #1) to activate the MG and TA muscles while attempting to grasp the item during the first 2 weeks post-lesion ($P < 0.001$; Fig. 12A, 0% success). The same muscles were reciprocally activated during stepping in the same animal as early as 1 week post-lesion (Fig. 8, left). On week 4 post-lesion, sequential, coordinated activation of the MG and TA muscles re-appeared during the grasping task, although the amplitude of muscle activity (Fig. 12B) remained smaller ($P < 0.001$) than pre-lesion. Successful retrieval of items at week 12 post-lesion (83%) was associated with coordinated activation of ankle antagonist muscles, with the level of TA EMG activity being similar to

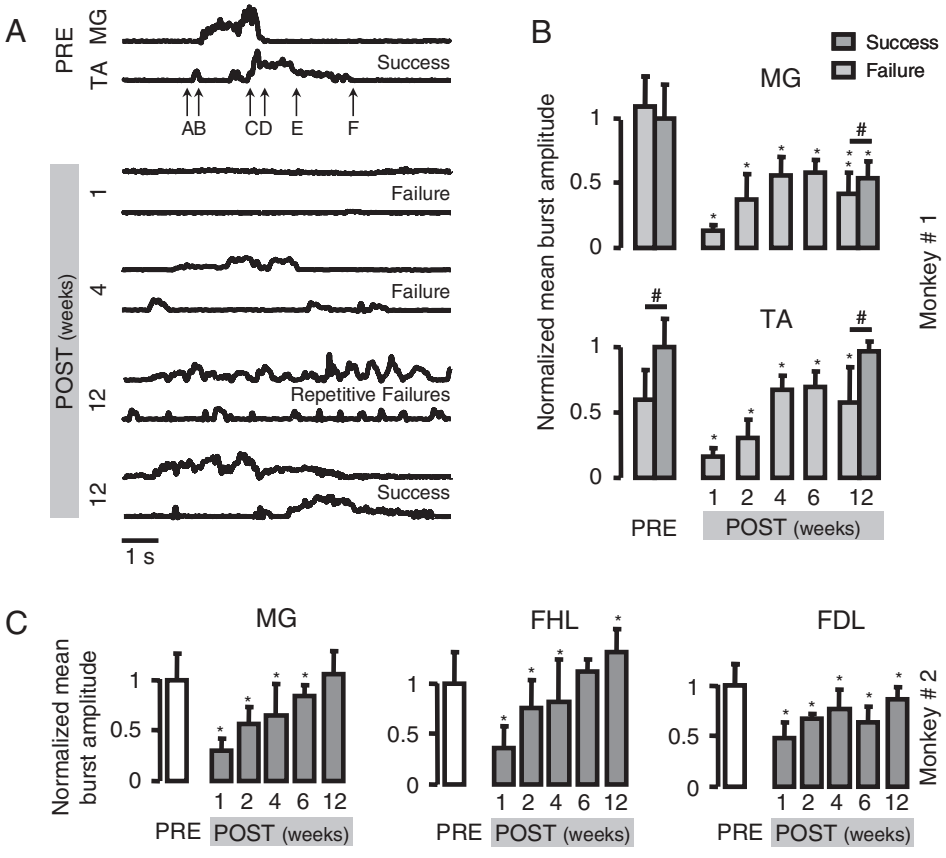

Fig. 12 (**A**) Typical rectified EMG activity recorded from MG and TA muscles in monkey #1 during performance of the retrieval task with the foot ipsilateral to the lesion at different time points. The result of the represented trial, i.e. success or failure, is indicated. The arrows labelled A–F point out different EMG events (see text for details). The amplitude scale is the same for all EMG traces. (**B**) Mean value (SD) of the amplitude of MG and TA muscle activity in monkey #1 pre-lesion and 1, 2, 4, 6 and 12 weeks post-lesion. Dark and light histogram bars differentiate success and failure trials, respectively. (**C**) Mean value (SD) of the amplitude of MG, FHL and FDL muscle activity in monkey #2 pre-lesion and 1, 2, 4, 6 and 12 weeks post-lesion. Asterisk and hash indicates significant difference (*t*-test) between pre- and post-lesion values and between failure and success trials, respectively.

pre-lesion (Fig. 12B). The mean amplitude of TA EMG activity, in turn, was weaker during failure compared to successful trials at week 12 post-lesion ($P < 0.001$), as observed pre-lesion during failure trials ($P < 0.001$). Fig. 12A (12 weeks, failure traces) clearly shows the weak EMG activity recorded while the monkey repeatedly tried to grasp the item and lift it from the platform.

Some (27%) of the CST fibres were spared in monkey #2, and, accordingly, successful trials (25%) were observed as early as 1 week post-lesion. Nonetheless, a decrease ($P < 0.001$ for all muscles) in the level of EMG activity was observed in the muscles in the HL ipsilateral to the lesion (Fig. 12C). The levels of EMG activity gradually increased in the MG and FHL muscles over the duration of the recovery period, and were similar to the pre-lesion baseline at week 6 (FHL) and 12 (MG) post-lesion. The level of EMG activity also increased progressively in the FDL muscle, but remained weaker ($P < 0.01$) at week 12 post-lesion compared to pre-lesion.

Discussion

A unilateral interruption of the fibres descending in the dorsolateral thoracic spinal cord in the monkey induced sustained locomotor deficits and abolished the ability to retrieve items with the foot. Although some control of the distal foot musculature was recovered, fine foot grasping remained significantly impaired even at 3 months post-lesion. These findings suggest that the CST normally makes an important contribution to interlimb and intralimb coordination during basic locomotion, as well as to the activation of specific muscles required to produce dexterous foot digit movements in the monkey. Furthermore, the present study reveals that the primate CNS has the ability to rapidly accommodate to a reduction in supraspinal control of locomotion, and to a less degree, fine foot motor skills.

Lesion of the thoracic dorsolateral column in the primate spinal cord

We successfully severed most of the fibres descending in the dorsolateral thoracic spinal cord white matter in the five out of the six monkeys tested (Figs 1 and 2). Most of the lumbar CST projections originating from the contralateral cerebral hemisphere, therefore, were interrupted, together with the uncrossed fibres from the ipsilateral motor cortex (~10%). Therefore, on the ipsilateral side only ventral (~1%) CST fibres were left intact by the lesion (Lacroix *et al.*, 2004). We could not exclude, however, that part of the red nucleus input which also was interrupted since the rubrospinal fibres descend in the lateral fasciculus in close proximity to CST axons (Kuypers, 1981). The red nucleus has a significant influence on motor neuron activity during generation of voluntary movements in the monkey (Lawrence and Kuypers, 1968*b*; Cheney *et al.*, 1991), and studies in cats showed that it may have a function similar to the motor cortex during walking (Rho *et al.*, 1999; Lavoie and Drew, 2002). Depending upon the monkey, the lesion also could have interrupted the spinocerebellar tract, part of the dorsal column and/or some propriospinal pathways. Each of these ascending and descending pathways potentially contribute to locomotor and fine motor functions. We suggest, however, that the observed motor impairments were primarily due to the interruption of the CST projections because alterations of monkey gait and foot grasping were consistent among the animals, regardless of the extent of the damage to the other pathways mentioned above. The major variations in the lesion extent and the associated differences in the recovery of function between the animals will be discussed in more detail in the next sections.

Role of cortical input in the control of monkey quadrupedal stepping

The most visible locomotor deficit produced by the CST lesion was the inability of the monkeys to properly initiate the swing phase of gait in the HL ipsilateral to the lesion. As a consequence, post-lesion, the HL cycle duration significantly increased (Fig. 7), and the limb endpoint overshot the position at which the forward oscillation was elicited during pre-lesion walking (Fig. 4). In two out of the three monkeys tested for locomotor ability, the failure to initiate the forward limb oscillation was associated with a dragging of the hindpaw along the treadmill belt during most of the swing phase (Fig. 3A). This foot drop was the behavioural expression of combined deficits in intralimb coupling (Figs. 3B, 4 and 5), notably between the knee and hip joints, and the inability to fully dorsiflex the foot and toes at the end of stance (Fig. 1B). Furthermore, the CST lesion produced systematic changes in the slope of the relationship between the stance/swing duration and the step cycle duration (Fig. 7, Table 3). These modifications of the gait cycle structure were reflected in the alteration in the temporal characteristics of extensor and flexor muscle recruitment (Fig. 8, Table 3). Such deficits in the spatial and temporal characteristics of limb oscillation and related muscle activation patterns suggest that the motor cortex (and possibly the red nucleus) plays an important role in terminating the period of extensor muscle activity during stance, and initiating the activity of flexor muscle activity for swing. Accordingly, Armstrong and Drew (1985) showed that stimulation of pyramidal cells in the walking cat enhances flexor muscle activity, and resets the locomotor rhythm, i.e. initiates a new period of swing (see also Rho *et al.*, 1999; Bretzner and Drew, 2005). This observation suggests that the motor cortex can act directly on the inter-neuronal spinal population that can modulate the timing of extensor and flexor motor neuron activation. Most likely, the basic locomotor rhythm emerges in monkeys, as in cats, from the integration of a centrally generated spinal rhythm (Grillner and Zangger, 1979), the limb afferent input from load-related (Duysens and Pearson, 1980) and hip extensor muscle mechanoreceptors (Grillner and Rossignol, 1978), and

descending signals (Shik *et al.*, 1966; Drew *et al.*, 2004). Furthermore, the impairment in intralimb coordination (Fig. 5) supports the view that the CST serves a role in modulating the temporal pattern of activity between flexor muscles acting at different joints (Jiang and Drew, 1996), perhaps, via the multi-segmental branching of cortical projections (Drew *et al.*, 2002).

Lesion of the dorsolateral thoracic spinal cord also provoked a systematic disruption in interlimb coordination (Fig. 10). Indeed, there is evidence that ascending, descending, and propriospinal pathways conjointly contribute to the regulation of the coordination between the limbs (review in Grillner, 1981), and that damage to any one of these neural components will change the normal interlimb coupling (Miller *et al.*, 1975; Kato *et al.*, 1984; Jankowska and Edgley, 1993; Jiang and Drew, 1996; Brustein and Rossignol, 1998). In the present study, interruption of the CST, spinocerebellar tracts and some propriospinal pathways (Miller *et al.*, 1975; English, 1985; Vilensky *et al.*, 1992; Jiang and Drew, 1996) most likely contributed to the severe alteration of interlimb coordination. It is important to note, however, that the monkeys (#1 and #2) eventually recovered a diagonal-couplet interlimb timing (Fig. 10), thereby suggesting that the motor cortex may not be an essential structure for ensuring primate-specific interlimb coordination during locomotion.

Comparisons with studies performed in subprimate animal models and relevance for SCI

Cats that receive a thoracic lesion of the lateral and dorsal descending pathways exhibit a prominent hindpaw drag during swing, an increased HL cycle duration, a disruption of stance/swing transition, an alteration in intralimb coupling, and a severe interlimb uncoupling (Jiang and Drew, 1996), features that are comparable to those detected in the present study in the monkey after a unilateral CST lesion. Rats show a 'complete' recovery of locomotor function within a day after a CST lesion (Muir and Whishaw, 1999). These inter-species differences are consistent with the view that that the development of the CST that accompanied mammalian evolution correlates with an increasingly important role of the motor cortex in controlling the spinal circuitry that generates the motor pattern for walking. A number of studies indeed have suggested that activation of stepping-related spinal circuits depends more on supraspinal input in non-human primates than in sub-primate mammals (Eidelberg *et al.*, 1981; Fedirchuk *et al.*, 1998; Vilensky and O'Connor, 1998). Nevertheless, similar behavioural deficits in cats and monkeys after a CST lesion suggest that the mechanism by which cortical input is integrated within the stepping-related spinal circuits do not differ qualitatively between the feline and primate. There are substantial differences, however, in the effects of a CST lesion in rats compared to the monkeys, emphasizing the importance of understanding the potential for neural regeneration strategies to mediate recovery of motor function in non-human primates before applying them to humans.

Role of the cortical input in the production of dexterous foot grasping movements

The unilateral CST lesion completely abolished the ability of four out of six monkeys to retrieve items with the ipsilateral foot during the first 2 weeks post-lesion (Fig. 11); there was a significant relationship between the total number of retrievals by the ipsilateral foot and the percentage of surviving CST axon (Fig. 11B), as observed following similar lesion in rodents (Weidner *et al.*, 2001; Keyvan-Fouladi *et al.*, 2003). EMG recordings from monkey #1 showed that the ankle antagonist muscles remained virtually quiescent when the animal unsuccessfully attempted to grasp the item during the first week post-lesion (Fig. 12 A–B). The reduced level of muscle recruitment was not as dramatic in monkey #2, although a substantial drop in EMG amplitude was observed in all distal HL muscles during the first week post-lesion (Fig. 12C). This animal retained ~27% of the CST projections that, interestingly, mediated a sufficient degree of control over the motor pools innervating the distal muscles to successfully accomplish the required grasping task (25% success at week 1). Furthermore, the lesion probably interrupted a larger amount of rubrospinal fibres in monkey #1 compared to monkey #2 (Fig. 1). The level of the lesion (T10 versus T3 in monkeys #1 and #2, respectively) may also have influenced the extent of the behavioural deficits, as suggested in humans (Dietz and Colombo, 2004). Monkey #2, in turn, showed larger locomotor impairments than monkey #1, while a larger disruption of gait was observed in monkey #3. Differences in the damage to non-CST pathways, notably the propriospinal system in monkeys #2 and #3 compared to monkey #1 (see Fig. 1), may explain this apparent discrepancy between the behaviour of the three animals. These differences emphasize the importance of knowing the completeness of the lesion in interpreting the role of specific tracts in modulating motor performance (see comments in Jiang and Drew, 1996; Lemon, 2004). These results also are important since they suggest that there is sufficient plasticity of descending axons for regaining a significant level of motor control following an incomplete SCI (Sasaki *et al.*, 2004).

Previous investigations similarly reported that complete, bilateral interruption of the cortical projections to the spinal cord results in persistent deficits in fine manual motor skills of the FLs (Lawrence and Kuypers, 1968*a*; Porter and Lemon, 1993; Galea and Darian-Smith, 1997*b*) while rapid recovery of locomotor performance generally is observed (Lawrence and Kuypers, 1968*a*). Kuypers (1978) concluded that the development of the descending pathways from the brain in primates correlates with the capacity to activate specific motor pools, and, thereby, to highly fractionate the movements of the distal segments of the hand (review in Lemon *et al.*, 2004). In the present study, direct and quantitative comparisons of fine motor and locomotor performance of the HLs

lead to conclusions similar to previous reports based on FL movements. Indeed, the density of CST projections is higher within both the cervical and lumbar spinal cord segments in primates than sub-primates (Lacroix *et al.*, 2004). Our results, therefore, show that the CST projections in non-human primates mediate a high degree of control over both the hand and foot musculature. Invasion of arboreal habitats by early primates probably created the evolutionary demands for the increased cortical control of spinal motor circuits to ensure accurate positioning of the limbs and precise hand and foot grasping during locomotion along fine-branches (Georgopoulos and Grillner, 1989; Schmitt, 2003).

Interestingly, the unilateral interruption of the CST modestly affected the fine grasping ability of the contralateral as well as the ipsilateral foot. Such bilateral effects might reflect the fact that ~10% of the CST axons descend within the ipsilateral dorsolateral column in monkeys, with most ipsilaterally projecting axons terminating within Rexed lamina IX, i.e. in close proximity to motoneuronal soma (Lacroix *et al.*, 2004). Moreover, Edgley *et al.* (2004) recently showed that pyramidal tract neurons exert a facilitating action on ipsilateral HL motor neurons via commissural interneurons. The observed bilateral impairments resulting from a unilateral CST lesion thus reveal that a single motor cortex may contribute to bilateral control of spinal motor neurons.

Effects of CST lesion on locomotion versus fine motor task

Interruption of the cortical projections to the lumbar spinal cord segments did not prevent the monkeys from walking quadrupedally on the treadmill for extended periods as early as 1 week post-lesion, although it completely abolished their ability to achieve skilled movements with the foot. Following the unilateral thoracic CST lesion, monkey #1 was no longer able to recruit motor pools innervating distal HL muscles when attempting to grasp food items (Fig. 12A), but, strikingly, showed a reciprocal, coordinated activation pattern of the same muscles during quadrupedal stepping at the same post-lesion time (Fig. 8). Clearly, this difference in motor neuron recruitment shows that the CST is a normal and necessary route to convey motor commands to the spinal motor infrastructure for the production of skilled HL movements in non-human primates (Lawrence and Kuypers, 1968b), while the other descending systems are sufficient to properly activate the spinal interneuronal population that drives motor neuron activity during monkey locomotion (Fedirchuk *et al.*, 1998), at least after sufficient accommodation has been allowed to occur. Indeed, Eidelberg *et al.* (1981) reported that stimulation of the posterior subthalamic region could elicit locomotor movements in thalamic monkeys. Likewise, Lawrence and Kuypers (1968b) suggested that the ventral pathways, compared to the pyramidal tracts, are of major importance to the production of locomotion in monkeys. In contrast, in human patients Nathan (1994) reported that bilateral interruption of the dorsolateral pathways abolished the ability to walk, whereas a bilateral incision affecting only the ventral pathways (lateral CST intact on both sides) left patients fully able to walk. Nonetheless, the effect of selective ventral pathway interruption on monkey locomotion has never been assessed, and therefore, the functional contribution of the CST to walking in humans compared to non-human primates remains unclear.

Spontaneous plasticity of the primate motor system in response to a unilateral SCI

The HL contralateral to the lesion side and both FLs showed a general response to the unilateral CST lesion during treadmill locomotion that is typical in quadrupeds (Lawrence and Kuypers, 1968*a*; Helgren and Goldberger, 1993; Webb and Muir, 2003) and bipeds (Wagenaar and Beek, 1992; Muir *et al.*, 1998). For example, stance duration (Fig. 7) and the intensity of muscle activity (Fig. 9) increased due to the inability of the ipsilateral HL to fully contribute to body weight support and propulsion. Nonetheless, the asymmetry in HL stepping movements almost vanished over the duration of the recovery period (12 weeks), and was associated with progressive improvement of interlimb (Fig. 10) and intralimb coordination (Fig. 5). Such a rapid recovery of locomotor function emphasizes the ability of the primate CNS to accommodate rapidly to a reduction in corticospinal control. In contrast, Drew *et al.* (2002) reported that, even following a mostly-unilateral lesion of the dorsolateral column, cats exhibited a slow and incomplete recovery of their stepping ability. These species-specific responses may suggest that the neuromotor system has a greater plasticity in monkeys than cats. Nevertheless, some kinematic features remained significantly impaired in monkeys during locomotion (Fig. 3B). Such deficiencies suggest that the integrity of the descending pathways from the brain is necessary for full expression of the monkey locomotor repertoire, although these features may have eventually subsided. Interestingly, the muscle synergies underlying the successful restoration of locomotion kinematics after the CST lesion (Fig. 3B) significantly differed from those recorded pre-lesion (Figs 8 and 9). Also, it may be important that significant muscle atrophy remained (unpublished data). Thus, it appears that recovery of walking was not achieved through the regeneration of normal neural connections, but involved a substantial re-organization of spinal and/or supraspinal circuit activation, as observed in cats (Jiang and Drew, 1996; Brustein and Rossignol, 1998; de Leon *et al.*, 2001; Tillakaratne *et al.*, 2002) and humans (Harkema, 2001; Grasso *et al.*, 2004) following SCI. The monkeys also demonstrated substantial, although incomplete, recovery in their ability to retrieve items with their feet, and this was associated with recovery of coordinated activation of the HL muscles (Fig. 12). Similarly, Sasaki *et al.* (2004) recently reported a significant recovery in dexterous finger movements following a unilateral lesion of the lateral CST in the cervical (C4/C5) spinal cord of monkeys.

A number of neural mechanisms may account for the rapid and substantial recovery of motor function following the unilateral interruption of the thoracic dorsolateral column observed in the present study. The identified potential mechanisms (reviewed in Raineteau and Schwab, 2001) include cortical reorganization (Nudo and Milliken, 1996; Marshall *et al.*, 2000; Schmidlin *et al.*, 2004), subcortical plasticity (Belhaj-Saif and Cheney, 2000), collateral sprouting of undamaged descending pathways (Weidner *et al.*, 2001; Raineteau *et al.*, 2002; Havton *et al.*, 2004), formation of new intraspinal circuits (Bareyre *et al.*, 2004), plasticity of stepping-related spinal interneuronal circuits (Rossignol *et al.*, 2002; Tillakaratne *et al.*, 2002; Edgerton *et al.*, 2004) and synaptic plasticity of afferent terminals arising from limb sensors (Helgren and Goldberger, 1993; Cote *et al.*, 2003; Gomez-Pinilla *et al.*, 2004). A mosaic of synaptic and anatomical plasticity, i.e. reorganization of pre-existing circuits and appearance of new connections, undoubtedly underlies the observed recovery of motor function. Since the present results show a significant capacity of the primate adult lesioned motor system for adaptive reorganization following SCI, it will be important to identify the actual neurobiological substrates to which the observed functional recovery can be attributed.

One of the aims of the present study was to develop a primate model of SCI that produced persistent deficits in locomotion and fine motor tasks, and in which neural repair interventions could be tested. We interrupted the CST because of the obvious relevance of this pathway in the human neuromotor organization (Porter and Lemon, 1993; Nathan, 1994), and since such lesions have been used in rodents (Weidner *et al.*, 2001; Raineteau *et al.*, 2002; Keyvan-Fouladi *et al.*, 2003). Unilateral CST lesions were utilised to spare autonomic function, minimize discomfort, and facilitate post-operative clinical management of the lesioned subjects. However, the substantial and rapid recovery of locomotor and fine motor function after this lesion has to be factored in when testing the effectiveness of interventions assumed to promote spinal cord regeneration, sprouting, or any other mechanism of neural reorganization. For testing sprouting mechanisms as a means of recovery from moderately severe injuries the present model has many advantages. For examining interventions designed to induce regeneration, increasing the extent of the injury and/or performing the lesion at the cervical rather than thoracic level may be necessary to assess the effectiveness of rehabilitative interventions (Courtine *et al.*, 2004; Yang *et al.*, 2004).

Conclusions

The present results demonstrate that the primary motor cortex has a significant effect on stepping-related spinal circuits even during unobstructed walking, and plays an important role in controlling locomotion in the monkey. Lesion-induced disruption of foot grasping ability also confirmed that the CST arising from the contralateral primary motor cortex is a main route through which volitional distal foot movements are controlled in the non-human primate as previously shown for the FL (Porter and Lemon, 1993). Furthermore, these data suggest that both the left and right lateral CSTs may conjointly contribute to fine motor function of each HL. Nonetheless, the substantial recovery observed in locomotion and fine motor control of the foot in the monkey after a SCI emphasizes the high degree of plasticity of the primate CNS. Given a better understanding of the mechanisms mediating this plasticity, the potential for neural repair strategies to enhance such spontaneous plasticity will be greatly augmented (Yang *et al.*, 2004). The difference in the level of repair that seems to occur in the more proximal versus the distal musculature, and in the more automated locomotor movements versus the tasks requiring fractionated control of distal digits are factors that should be considered in any attempts to apply techniques to re-establish functional connectivity after a SCI or a loss of brain function.

Acknowledgements

Supported by the National Institutes of Health (Grant Number: RO1-NS42291) and the California Roman Reed Bill.

References

Anderson KD. Targeting recovery: priorities of the spinal cord-injured population. J Neurotrauma 2004; 21: 1371–83.

Armstrong DM, Drew T. Forelimb electromyographic responses to motor cortex stimulation during locomotion in the cat. J Physiol 1985; 367: 327–51.

Bareyre FM, Kerschensteiner M, Raineteau O, Mettenleiter TC, Weinmann O, Schwab ME. The injured spinal cord spontaneously forms a new intraspinal circuit in adult rats. Nat Neurosci 2004; 7: 269–77.

Belhaj-Saif A, Cheney PD. Plasticity in the distribution of the red nucleus output to forearm muscles after unilateral lesions of the pyramidal tract. J Neurophysiol 2000; 83: 3147–53.

Bonnard M, Camus M, Coyle T, Pailhous J. Task-induced modulation of motor evoked potentials in upper-leg muscles during human gait: a TMS study. Eur J Neurosci 2002; 16: 2225–30.

Bretzner F, Drew T. Contribution of the motor cortex to the structure and the timing of hindlimb locomotion in the cat: a microstimulation study. J Neurophysiol 2005.

Brustein E, Rossignol S. Recovery of locomotion after ventral and ventrolateral spinal lesions in the cat. I. Deficits and adaptive mechanisms. J Neurophysiol 1998; 80: 1245–67.

Capaday C, Lavoie BA, Barbeau H, Schneider C, Bonnard M. Studies on the corticospinal control of human walking. I. Responses to focal transcranial magnetic stimulation of the motor cortex. J Neurophysiol 1999; 81: 129–39.

Cheney PD, Fetz EE, Mewes K. Neural mechanisms underlying corticospinal and rubrospinal control of limb movements. Prog Brain Res 1991; 87: 213–52.

Cote MP, Menard A, Gossard JP. Spinal cats on the treadmill: changes in load pathways. J Neurosci 2003; 23: 2789–96.

Courtine G, Schieppati M. Tuning of a basic coordination pattern constructs straight-ahead and curved walking in humans. J Neurophysiol 2004; 91: 1524–35.

Courtine G, Hodgson JA, Raven J, Roy RR, McKay H, Bernot T, et al. Effects of a unilateral corticospinal tract (CST) lesion or a complete cervical hemisection (HS) on locomotor performance in a primate. Washington D.C. Soc Neurosci 2004. Program No. 654.657.

Courtine G, Roy RR, Hodgson JA, McKay H, Raven J, Zhong H, et al. Kinematic and EMG determinants in quadrupedal locomotion of a non-human primate (monkeys). J Neurophysiol 2005; 93: 3127–45.

de Leon RD, Roy RR, Edgerton VR. Is the recovery of stepping following spinal cord injury mediated by modifying existing neural pathways or by generating new pathways? A perspective. Phys Ther 2001; 81: 1904–11.

Dietz V, Colombo G. Recovery from spinal cord injury—underlying mechanisms and efficacy of rehabilitation. Acta Neurochir Suppl 2004; 89: 95–100

Drew T, Jiang W, Widajewicz W. Contributions of the motor cortex to the control of the hindlimbs during locomotion in the cat. Brain Res Brain Res Rev 2002; 40: 178–91.

Drew T, Prentice S, Schepens B. Cortical and brainstem control of locomotion. Prog Brain Res 2004; 143: 251–61.

Duysens J, Pearson KG. Inhibition of flexor burst generation by loading ankle extensor muscles in walking cats. Brain Res 1980; 187: 321–32.

Duysens J, Van de Crommert HW. Neural control of locomotion; the central pattern generator from cats to humans. Gait Posture 1998; 7: 131–41.

Edgerton VR, Roy RR. Paralysis recovery in humans and model systems. Curr Opin Neurobiol 2002; 12: 658–67.

Edgerton VR, Tillakaratne NJ, Bigbee AJ, de Leon RD, Roy RR. Plasticity of the spinal neural circuitry after injury. Annu Rev Neurosci 2004; 27: 145–67.

Edgley SA, Jankowska E, Hammar I. Ipsilateral actions of feline corticospinal tract neurons on limb motoneurons. J Neurosci 2004; 24: 7804–13.

Eidelberg E, Walden JG, Nguyen LH. Locomotor control in macaque monkeys. Brain 1981; 104: 647–63.

English AW. Interlimb coordination during stepping in the cat: the role of the dorsal spinocerebellar tract. Exp Neurol 1985; 87: 96–108.

Fedirchuk B, Nielsen J, Petersen N, Hultborn H. Pharmacologically evoked fictive motor patterns in the acutely spinalized marmoset monkey (*Callithrix jacchus*). Exp Brain Res 1998; 122: 351–61.

Fukuyama H, Ouchi Y, Matsuzaki S, Nagahama Y, Yamauchi H, Ogawa M, et al. Brain functional activity during gait in normal subjects: a SPECT study. Neurosci Lett 1997; 228: 183–6.

Galea MP, Darian-Smith I. Multiple corticospinal neuron populations in the macaque monkey are specified by their unique cortical origins, spinal terminations, and connections. Cereb Cortex 1994; 4: 166–94.

Galea MP, Darian-Smith I. Corticospinal projection patterns following unilateral section of the cervical spinal cord in the newborn and juvenile macaque monkey. J Comp Neurol 1997a; 381: 282–306.

Galea MP, Darian-Smith I. Manual dexterity and corticospinal connectivity following unilateral section of the cervical spinal cord in the macaque monkey. J Comp Neurol 1997b; 381: 307–19.

Georgopoulos AP, Grillner S. Visuomotor coordination in reaching and locomotion. Science 1989; 245: 1209–10.

Gomez-Pinilla F, Ying Z, Roy RR, Hodgson J, Edgerton VR. Afferent input modulates neurotrophins and synaptic plasticity in the spinal cord. J Neurophysiol 2004; 92: 3423–32.

Grasso R, Ivanenko YP, Zago M, Molinari M, Scivoletto G, Castellano V, et al. Distributed plasticity of locomotor pattern generators in spinal cord injured patients. Brain 2004; 127: 1019–34.

Grillner S. Control of locomotion in biped, tetrapod and fish. In: Handbook of physiology. The nervous system II. Bethesda MD: American Physiological physiology; 1981. p. 1179–236.

Grillner S, Rossignol S. On the initiation of the swing phase of locomotion in chronic spinal cats. Brain Res 1978; 146: 269–77.

Grillner S, Zangger P. On the central generation of locomotion in the low spinal cat. Exp Brain Res 1979; 34: 241–61.

Harkema SJ. Neural plasticity after human spinal cord injury: application of locomotor training to the rehabilitation of walking. Neuroscientist 2001; 7: 455–68.

Havton LA, Yang H, McKay H, Hodgson JA, Bernot T, Raven J, et al. Plasticity of the corticospinal tract in a primate spinal cord injury model. Washington D.C. Soc Neurosci 2004. Program No. 185.110.

Helgren ME, Goldberger ME. The recovery of postural reflexes and locomotion following low thoracic hemisection in adult cats involves compensation by undamaged primary afferent pathways. Exp Neurol 1993; 123: 17–34.

Hodgson JA, Wichayanuparp S, Recktenwald MR, Roy RR, McCall G, Day MK, et al. Circadian force and EMG activity in hindlimb muscles of monkeys. J Neurophysiol 2001; 86: 1430–44.

Jankowska E, Edgley S. Interactions between pathways controlling posture and gait at the level of spinal interneurones in the cat. Prog Brain Res 1993; 97: 161–71.

Jiang W, Drew T. Effects of bilateral lesions of the dorsolateral funiculi and dorsal columns at the level of the low thoracic spinal cord on the control of locomotion in the adult cat. I. Treadmill walking. J Neurophysiol 1996; 76: 849–66.

Jones LL, Oudega M, Bunge MB, Tuszynski MH. Neurotrophic factors, cellular bridges and gene therapy for spinal cord injury. J Physiol 2001; 533: 83–9.

Kato M, Murakami S, Yasuda K, Hirayama H. Disruption of fore- and hindlimb coordination during overground locomotion in cats with bilateral serial hemisection of the spinal cord. Neurosci Res 1984; 2: 27–47.

Keyvan-Fouladi N, Raisman G, Li Y. Functional repair of the corticospinal tract by delayed transplantation of olfactory ensheathing cells in adult rats. J Neurosci 2003; 23: 9428–34.

Kuypers HG. The motor system and the capacity to execute highly fractionated distal extremity movements. Electroencephalogr Clin Neurophysiol Suppl 1978; 34: 429–31.

Kuypers HG. Anatomy of the descending pathways. In: Brooks VB, Brookhart JM, Mountcastle VB, editors. Handbook of physiology. Section 1: The Nervous System, Vol 2. Bethesda, MD: Amercian Physiological Society; 1981. p. 597–666.

Lacquaniti F, Ivanenko YP, Zago M. Kinematic control of walking. Arch Ital Biol 2002; 140: 263–72.

Lacroix S, Havton LA, McKay H, Yang H, Brant A, Roberts J, et al. Bilateral corticospinal projections arise from each motor cortex in the macaque monkey: a quantitative study. J Comp Neurol 2004; 473: 147–61.

Lavoie S, Drew T. Discharge characteristics of neurons in the red nucleus during voluntary gait modifications: a comparison with the motor cortex. J Neurophysiol 2002; 88: 1791–814.

Lawrence DG, Kuypers HG. The functional organization of the motor system in the monkey. I. The effects of bilateral pyramidal lesions. Brain 1968a; 91: 1–14.

Lawrence DG, Kuypers HG. The functional organization of the motor system in the monkey. II. The effects of lesions of the descending brain-stem pathways. Brain 1968b; 91: 15–36.

Lemon R. Cortico-motoneuronal system and dexterous finger movements. J Neurophysiol 2004; 92: 3601; author reply 3601–3.

Lemon RN, Kirkwood PA, Maier MA, Nakajima K, Nathan P. Direct and indirect pathways for corticospinal control of upper limb motoneurons in the primate. Prog Brain Res 2004; 143: 263–79.

Liddell E, Phillips C. Pyramidal section in the cat. Brain 1944; 67: 1–9.

Marshall RS, Perera GM, Lazar RM, Krakauer JW, Constantine RC, DeLaPaz RL. Evolution of cortical activation during recovery from corticospinal tract infarction. Stroke 2000; 31: 656–61.

Miyai I, Tanabe HC, Sase I, Eda H, Oda I, Konishi I, et al. Cortical mapping of gait in humans: a near-infrared spectroscopic topography study. Neuroimage 2001; 14: 1186–92.

Miller S, Van Der Burg J, Van Der Meche F. Coordination of movements of the kindlimbs and forelimbs in different forms of locomotion in normal and decerebrate cats. Brain Res 1975; 91: 217–37.

Mori S, Miyashita E, Nakajima K, Asanome M. Quadrupedal locomotor movements in monkeys (M. fuscata) on a treadmill: kinematic analyses. Neuroreport 1996; 7: 2277–85.

Muir GD, Katz SL, Gosline JM, Steeves JD. Asymmetric bipedal locomotion—an adaptive response to incomplete spinal injury in the chick. Exp Brain Res 1998; 122: 275–82.

Muir GD, Whishaw IQ. Complete locomotor recovery following corticospinal tract lesions: measurement of ground reaction forces during overground locomotion in rats. Behav Brain Res 1999; 103: 45–53.

Nakajima K, Mori F, Takasu C, Mori M, Matsuyama K, Mori S. Biomechanical constraints in hindlimb joints during the quadrupedal versus bipedal locomotion of M. fuscata. Prog Brain Res 2004; 143: 183–90.

Nathan PW. Effects on movement of surgical incisions into the human spinal cord. Brain 1994; 117: 337–46.

Nudo RJ, Milliken GW. Reorganization of movement representations in primary motor cortex following focal ischemic infarcts in adult squirrel monkeys. J Neurophysiol 1996; 75: 2144–9.

Petersen NT, Butler JE, Marchand-Pauvert V, Fisher R, Ledebt A, Pyndt HS, et al. Suppression of EMG activity by transcranial magnetic stimulation in human subjects during walking. J Physiol 2001; 537: 651–6.

Poppele R, Bosco G. Sophisticated spinal contributions to motor control. Trends Neurosci 2003; 26: 269–76.

Porter R, Lemon R. Corticospinal function and voluntary movement. Physiological Society Monograph, Number 45. Oxford: Oxford University Press; 1993.

Raineteau O, Fouad K, Bareyre FM, Schwab ME. Reorganization of descending motor tracts in the rat spinal cord. Eur J Neurosci 2002; 16: 1761–71.

Raineteau O, Schwab ME. Plasticity of motor systems after incomplete spinal cord injury. Nat Rev Neurosci 2001; 2: 263–73.

Recktenwald MR, Hodgson JA, Roy RR, Riazanski S, McCall GE, Kozlovskaya I, et al. Effects of spaceflight on monkeys quadrupedal locomotion after return to 1G. J Neurophysiol 1999; 81: 2451–63.

Rho MJ, Lavoie S, Drew T. Effects of red nucleus microstimulation on the locomotor pattern and timing in the intact cat: a comparison with the motor cortex. J Neurophysiol 1999; 81: 2297–315.

Rossignol S, Bouyer L, Barthelemy D, Langlet C, Leblond H. Recovery of locomotion in the cat following spinal cord lesions. Brain Res Brain Res Rev 2002; 40: 257–66.

Sasaki S, Isa T, Pettersson LG, Alstermark B, Naito K, Yoshimura K, et al. Dexterous finger movements in primate without monosynaptic corticomotoneuronal excitation. J Neurophysiol 2004; 92: 3142–7.

Schmitt D. Insights into the evolution of human bipedalism from experimental studies of humans and other primates. J Exp Biol 2003; 206: 1437–48.

Schwab ME. Repairing the injured spinal cord. Science 2002; 295: 1029–31.

Schmidlin E, Wannier T, Bloch J, Rouiller EM. Progressive plastic changes in the hand representation of the primary motor cortex parallel incomplete recovery from a unilateral section of the corticospinal tract at cervical level in monkeys. Brain Res 2004; 1017: 172–83.

Shik ML, Severin FV, Orlovskii GN. [Control of walking and running by means of electric stimulation of the midbrain]. Biofizika 1966; 11: 659–66.

Tillakaratne NJ, de Leon RD, Hoang TX, Roy RR, Edgerton VR, Tobin AJ. Use-dependent modulation of inhibitory capacity in the feline lumbar spinal cord. J Neurosci 2002; 22: 3130–43.

Tower SS. Pyramidal lesion in the monkey. Brain 1940; 63: 36–90.

Tuszynski MH, Grill R, Jones LL, McKay HM, Blesch A. Spontaneous and augmented growth of axons in the primate spinal cord: effects of local injury and nerve growth factor-secreting cell grafts. J Comp Neurol 2002; 449: 88–101.

Vilensky JA, Moore AM, Eidelberg E, Walden JG. Recovery of locomotion in monkeys with spinal cord lesions. J Mot Behav 1992; 24: 288–96.

Vilensky JA, O'Connor BL. Stepping in nonhuman primates with a complete spinal cord transection: old and new data, and implications for humans. Ann N Y Acad Sci 1998; 860: 528–30.

Wagenaar RC, Beek WJ. Hemiplegic gait: a kinematic analysis using walking speed as a basis. J Biomech 1992; 25: 1007–15.

Webb AA, Muir GD. Unilateral dorsal column and rubrospinal tract injuries affect overground locomotion in the unrestrained rat. Eur J Neurosci 2003; 18: 412–22.

Weidner N, Ner A, Salimi N, Tuszynski MH. Spontaneous corticospinal axonal plasticity and functional recovery after adult central nervous system injury. Proc Natl Acad Sci USA 2001; 98: 3513–8.

Yang H, McKay H, Hodgson JA, Bernot T, Raven J, Courtine G, et al. BDNF and NT3 gene delivry in models of primate spinal cord injury (SCI). Washington D.C. Soc Neurosci 2004. Program No. 106.14.